Water Research Laboratory

Never Stand Still | Faculty of Engineering | School of Civil and Environmental Engineering

3D Physical Modelling of Coffs Harbour Northern Breakwater Upgrade

WRL Technical Report 2015/05
May 2015

By F Flocard

Water Research Laboratory
UNSW Australia
School of Civil and Environmental Engineering

3D Physical Modelling of Coffs Harbour Northern Breakwater Upgrade

WRL Technical Report 2015/05
May 2015

by
F Flocard

Project Details

Report Title	3D Physical Modelling of Coffs Harbour Northern Breakwater Upgrade
Report Author(s)	F Flocard
Report No.	2015/05
Report Status	Final
Date of Issue	29/05/2015
WRL Project No.	2012109
Project Manager	Francois Flocard
Client Name	GHD
Client Address	Level 15, 133 Castlereagh Street Sydney NSW 2000
Client Contact	Mr Craig Dengate
Client Reference	

Document Status

Version	Reviewed By	Approved By	Date Issued
Draft	M J Blacka	G P Smith	20/05/2015
Final	M J Blacka	G P Smith	29/05/2015

Water Research Laboratory

110 King Street, Manly Vale, NSW, 2093, Australia

Tel: +61 (2) 8071 9800 Fax: +61 (2) 9949 4188

ABN: 57 195 873 179

www.wrl.unsw.edu.au

Quality System certified to AS/NZS ISO 9001:2008

Expertise, research and training for industry and government since 1959

A major group within water@UNSW water research centre

Contents

List of Tables

List of Figures

1. Introduction

The Water Research Laboratory (WRL) of the School of Civil and Environmental Engineering at UNSW Australia was commissioned by GHD on behalf of NSW Trade and Investment – Catchments and Lands (Crown Lands), to undertake three-dimensional (3D) physical modelling of the Coffs Harbour Northern Breakwater (Figure 1.1). Crown Lands is currently planning remedial works for the breakwater, with GHD undertaking the design of the upgraded breakwater. The 3D physical modelling program was required to assist the detailed design for the breakwater upgrade strategy. This report summarises the physical model design and scaling, test program, and findings of the study.

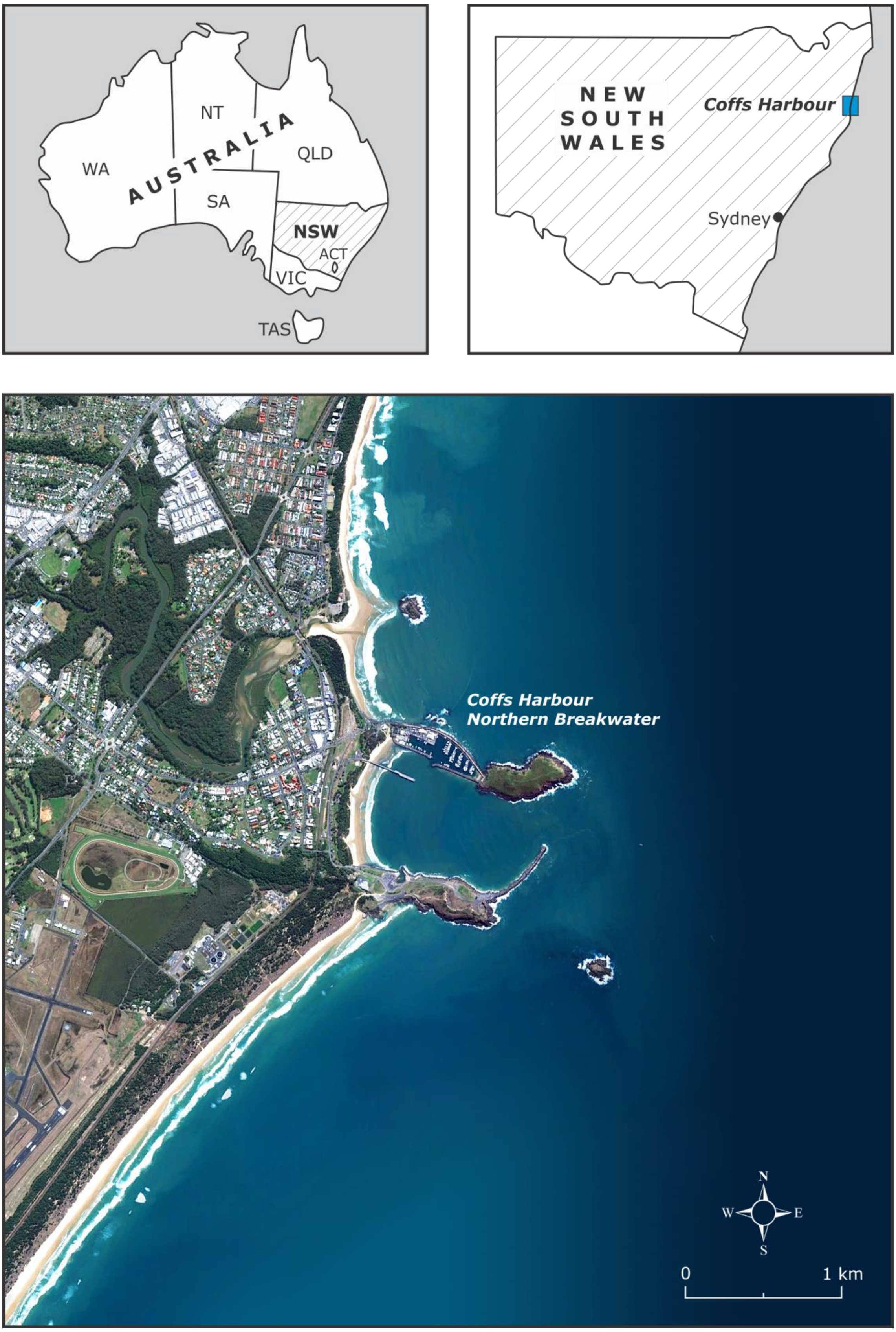

Figure 1.1: Location

2. Study Objectives

The key objectives of the 3D model study included:

- Assessment of nearshore wave breaking, shoaling and refraction processes;
- 3D armour stability assessment of the upgraded breakwater; and
- Analysis of 3D aspects of overtopping of the existing and upgraded breakwaters.

Prior to WRL undertaking the physical modelling, GHD had completed numerical SWAN (Simulating WAves Nearshore) and Boussinesq wave propagation modelling of the site. Based on WRL's experience, the numerical modelling is expected to have performed well at predicting the wave climate as waves approached the site through deeper water. However, in the nearshore area where waves diffract, refract, and break over specific bathymetric features, it is expected that the 3D physical model would more accurately simulate wave processes. The 3D physical model was therefore initially used to gain an understanding of the nearshore wave processes, and to provide a refined design wave climate directly in front of the Coffs Harbour Northern Breakwater.

The physical model validation involved a qualitative assessment of the overtopping to the breakwater in areas where this is known to be a major hazard (e.g. adjacent to the marina). Based on a recent survey of the existing structure performed by GHD, a model of the breakwater in its present state was initially developed and tested under two major historical storm events (2004 and 2009). The location and intensity of overtopping over the crest of the model was compared to photographic records taken during the two historical storm events.

Model testing of the proposed upgrade design option was then conducted under two different average recurrence interval (ARI) events (10 year and 100 year ARI). Separate tests were conducted to examine overtopping and armour stability.

3. Location and Design Conditions

3.1 Location

Coffs Harbour is located on the mid-north coast of NSW, as shown in Figure 1.1. While several coastal protection structures exist within the harbour, this investigation focused only on the Northern Breakwater. The site is typically exposed to open ocean waves from a north-east (NE) to east-south-east (ESE) direction.

3.2 Design Conditions

A range of "target" test conditions for the modelling were provided to WRL by GHD (GHD, 2014) and are reproduced in Table 3.1. The wave climate was estimated from numerical model predictions (not undertaken by WRL) and analysis of historical events (Watterson and Driscoll, 2011) with the conditions specified for a location approximately 1.5 wavelengths (195 m) seaward of the structure at chainage 480 m.

Table 3.1: "Target" Test Conditions for Three-Dimensional Modelling

Event Name	WL (m AHD)	Hs (m)	T_P (s)
2004 Storm	0.94	2.9	12.5
2009 Storm / 10 year ARI	1.20	4.8	12.5
100 year ARI MSL	0.00	4.8	15.3
100 year ARI HAT	1.20	5.4	15.3
100 year ARI HAT+ SLR	1.90	5.5	15.3

4. Three-dimensional Model Setup and Operation

4.1 Testing Facilities

All testing carried out in this study was undertaken in the 3D wave basin at WRL. This basin measures approximately 29 m in length, 16 m in width and 0.7 m in depth. The walls of the basin are constructed of rendered and sealed brickwork, on a permanent concrete floor. For this particular study, the bathymetry at the site was reproduced in the model to scale using recycled aggregate capped with fibre reinforced concrete. Temporary concrete brick guide walls were installed as required inside the wave basin, to assist refraction and propagation of the waves as they approached the test structure and reduce erroneous reflections in the basin. The required water level in the basin was set prior to each test using a scale mounted on the inner wall of the basin.

4.2 Wave Generation and Recording

Two wave paddles were used to generate waves in the wave basin. The twin piston type wave paddles are hydraulically driven by a 55 kW pump located in a separate building. Each wave paddle measures approximately 7.25 m in length and just over 1 m in height. The wave paddles and actuators are mounted on steel frames which are bolted to the concrete floor of the wave basin during tests. The paddles are moveable and able to be rotated to produce waves of varying approach angles to the test structure, though only a wave direction of 67.5° TN (ENE) was used for this study.

Wave data was collected at a range of locations in the basin using capacitance wave probes. High frequency water level data from the wave probes was recorded on a PC using the National Instruments LabVIEW software package, and the time series of water level data post processed to produce wave statistics for each location using the Mathworks MATLAB software package.

4.3 Model Design and Scaling

4.3.1 Introduction

Model scaling was based on geometric similarity between model and prototype, with an undistorted length scale of 58 being used for all tests. In designing the model and establishing the model scale, a range of parameters were taken into consideration such as:

- Optimising extent of bathymetry reproduced in model;
- Minimising scale effects for armour stability tests;
- Maximising area of Northern Breakwater extent reproduced in model;
- Ensuring target wave and water level conditions could be achieved; and
- Available model Hanbars armour unit sizes.

In considering these parameters, an undistorted length scale of 1:58 was selected for the model. The scaling relationship between length and time was determined by Froudian similitude, with the following scale ratios (prototype divided by model) being adopted:

- Length ratio $L_R = 58$
- Time ratio $T_R = L_R^{0.5} = 7.62$
- Velocity ratio $V_R = L_R^{0.5} = 7.62$
- Mass ratio $M_R = L_R^3 = 195,112$

4.3.2 *Armour Stability Scaling*

Although the stability of breakwater armour stones is able to be successfully modelled in a study such as this, scaling limitations as well as material properties prevent their material strengths from being modelled. The result is that the reaction of armour units or stones to abrasive and splitting forces applied in the real world structure is not able to be predicted by the physical modelling study, and as such the ability of individual armour units to maintain integrity cannot be predicted, though this was not one of the aims of the physical modelling.

Scale effects that alter armour stability behaviour can be introduced into the model if the flow conditions through the structure pores are altered such that fully turbulent conditions in the prototype become partially turbulent or laminar in the model. These scale effects can arise if the armour units or the water velocities in the model are too small. To avoid the occurrence of these scale effects, it is recommended in Shore Protection Manual (SPM) (1984, p7-208) that the Reynolds Number (Re) for flow through the primary armour layer exceeds 3×10^4, where Reynolds Number is determined using Equation 4.1.

$$\mathrm{Re} = \frac{(gH)^{\frac{1}{2}} k_\Delta}{\upsilon} \left(\frac{M_r}{\rho_r} \right)^{\frac{1}{3}} \tag{4.1}$$

where:
- H: Wave height
- M_r: Armour stone mass
- ρ_r: Armour stone density
- υ: Kinematic viscosity
- k_Δ: Layer coefficient.

However, Tirindelli *et al.* (2000) document the results of several scale effect studies with emergent rubble mound structures. These results are summarised as:

- Dai and Kamel (1969) tested rubble armour with D_{n50} = 20 – 300 mm (model scale) using regular waves and found no scale effects on armour layer damage for Re > 3×10^4
- Thompson and Shuttler (1975) tested irregular waves with model rock armour in the range of 20 – 40 mm, and showed no clear dependence of erosion on Re
- Torum et al. (1977), Broderick and Ahrens (1982), Mol *et al.* (1983), and Van der Meer (1988) investigated scale effects with irregular waves, and found no effects for Re in the range of 1×10^4 to 4×10^4
- Jensen and Klinting (1983) presented theoretical argument that scale effects are eliminated if Re > 0.7×10^4.

The data from Tirindelli *et al.* (2000) highlights that the boundary for the introduction of scale effects is not precise, and that the accepted Reynolds Number of 3×10^4 recommended in SPM (1984) is based on a very limited number of studies and is probably conservative. The equation for calculating Reynolds Numbers within the armour layer is a very simplistic approach, as the turbulence of armour layer flow is likely to be dependent on many more parameters than simply wave height, armour stone size, and viscosity. An example would be that a Hanbar armoured layer is more porous, rough, and angular than a rock layer, and therefore would likely result in higher turbulence compared to a rock layer. This is confirmed by the knowledge that Hanbar armoured slopes are more effective at dissipating wave energy than an equivalent rock armoured slope, due to their roughness and additional porosity. However, there is no parameter in the Reynolds Number equation presented in SPM (1984) to account for such factors.

Recent guidelines for physical modelling of rubble breakwater structures, Hydralab (2007), avoids the use of Reynolds Number criteria for considering model scale limitations, and instead lists a series of guideline values for model parameters:

- Water depth: > 50 mm;
- Wave height: > 20-30 mm, with design wave height > 50 mm;
- Wave period: restricted by realistic wave steepness;
- Rock diameter: 3-5 mm; and
- Rock armour: >25 mm.

Table 4.1 shows calculated values of Reynolds Number for different combinations of model armour size and wave height, as applied in physical model of the Coffs Harbour Northern breakwater. Also shown are the model armour stone diameters.

Table 4.1: Reynolds Numbers and Armour Sizes in Model

Prototype Armour Mass (T)	Armour Type	Model Armour Mass (g)	Armour Size Model[1] (mm)	Reynolds Number in Model for Indicated Wave Height				
				H=1 m	H=2 m	H=3 m	H=4 m	H=5 m
5-8	Rock	33	35	9.95E+03	1.41E+04	1.72E+04	1.99E+04	2.23E+04
10	Concrete Cube	51	40	1.15E+04	1.62E+04	1.99E+04	2.30E+04	2.57E+04
12	Hanbar	62	43	1.23E+04	1.74E+04	2.13E+04	2.46E+04	2.75E+04
20	Hanbar	103	51	1.46E+04	2.07E+04	2.53E+04	2.92E+04	3.27E+04

Note: (1) Armour size (model) has been determined as equivalent sphere diameter for rock armour and unit size length for Hanbar.

All criteria set out in Hydralab (2007) were satisfied, as the design wave heights used in this modelling investigation were at least 1.5 times the minimum recommended wave height of 50 mm. Likewise, design water depths in the model exceed the minimum depth required. All rock and concrete armouring is larger than the recommended 25 mm model size. For most aspects of the modelling, Reynolds Number criteria exceed those considered acceptable by most published data.

4.4 Model Construction

Using plan drawings of the breakwater site, a model scale coordinate system was set up for the area modelled within the wave basin. The coordinate system was established as a two dimensional X and Y coordinate system in the horizontal plane. All features of the model, such as location of the present northern breakwater structure, the bathymetric sections, and the wave measurement locations were able to be located within the model using this X and Y coordinate system. Photos showing the construction of the model are shown in Figure 4.1. Photos showing the completed model bathymetry and existing breakwater core are shown in Figure 4.2.

a) Preparation of Basin Floor

b) Aggregate being placed between Masonite Transects

c) Aggregate in place before Concrete Capping Pour

Figure 4.1: Bathymetry Construction (1/2)

a) Overview of finished concrete bathymetry

b) Overview of Existing Breakwater Core and of Muttonbird Island Shoreline with Increased Roughness

Figure 4.2: Bathymetry Construction (2/2)

4.4.1 Model Layout

The layout of the model within the wave basin was finalised after considering numerous options. Figure 4.3 and Figure 4.4 show the position of the wave basin relative to the site, as well as the layout of the modelled bathymetry and the wave basin facility respectively. The selected model layout allowed bathymetry that extended approximately 650 m (4 wavelengths) north-east of the existing breakwater. Three wavelengths is the minimum bathymetric extent seaward of model test structures recommended in Hydralab (2007).

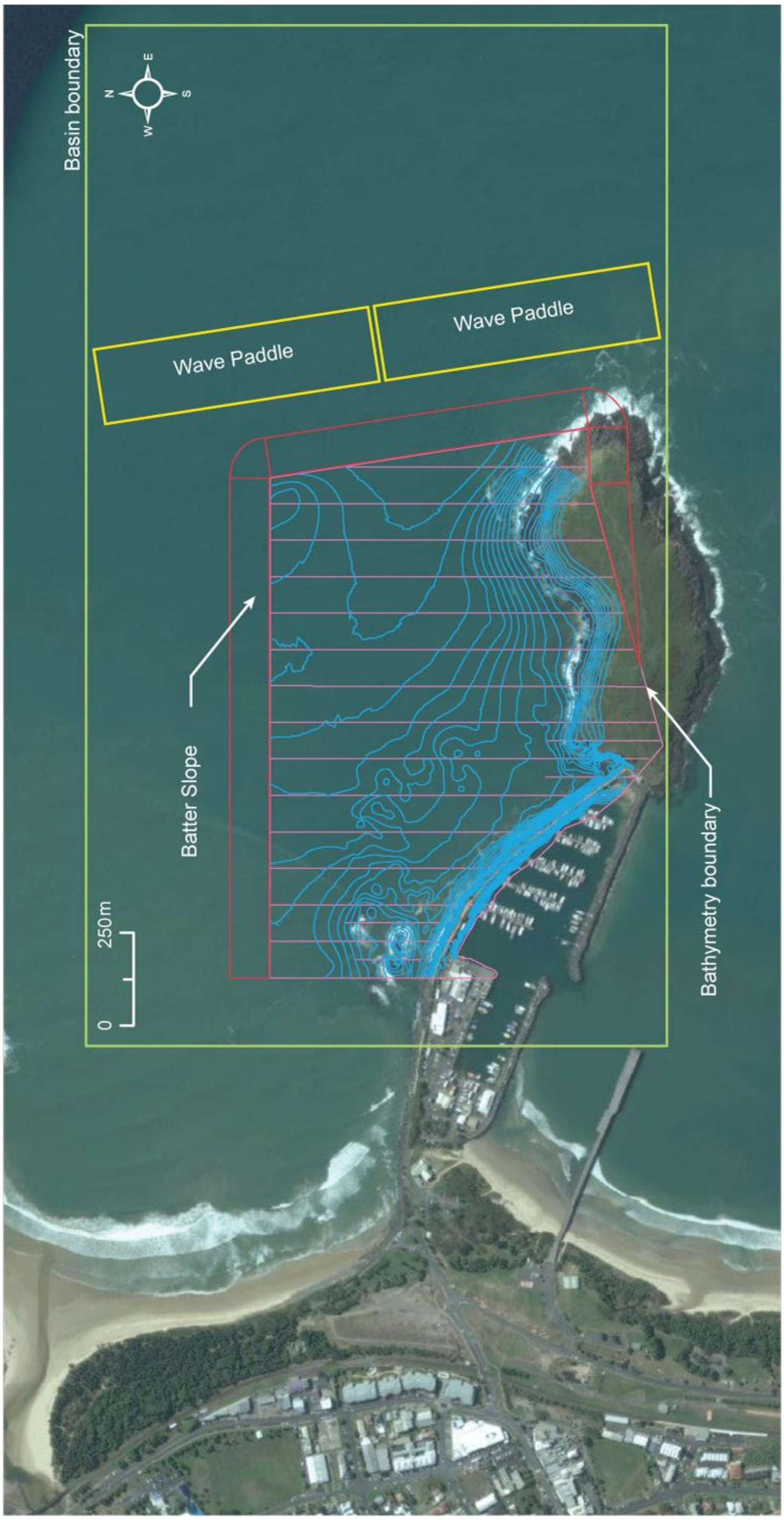

Figure 4.3: Position of Wave Basin Relative to Site

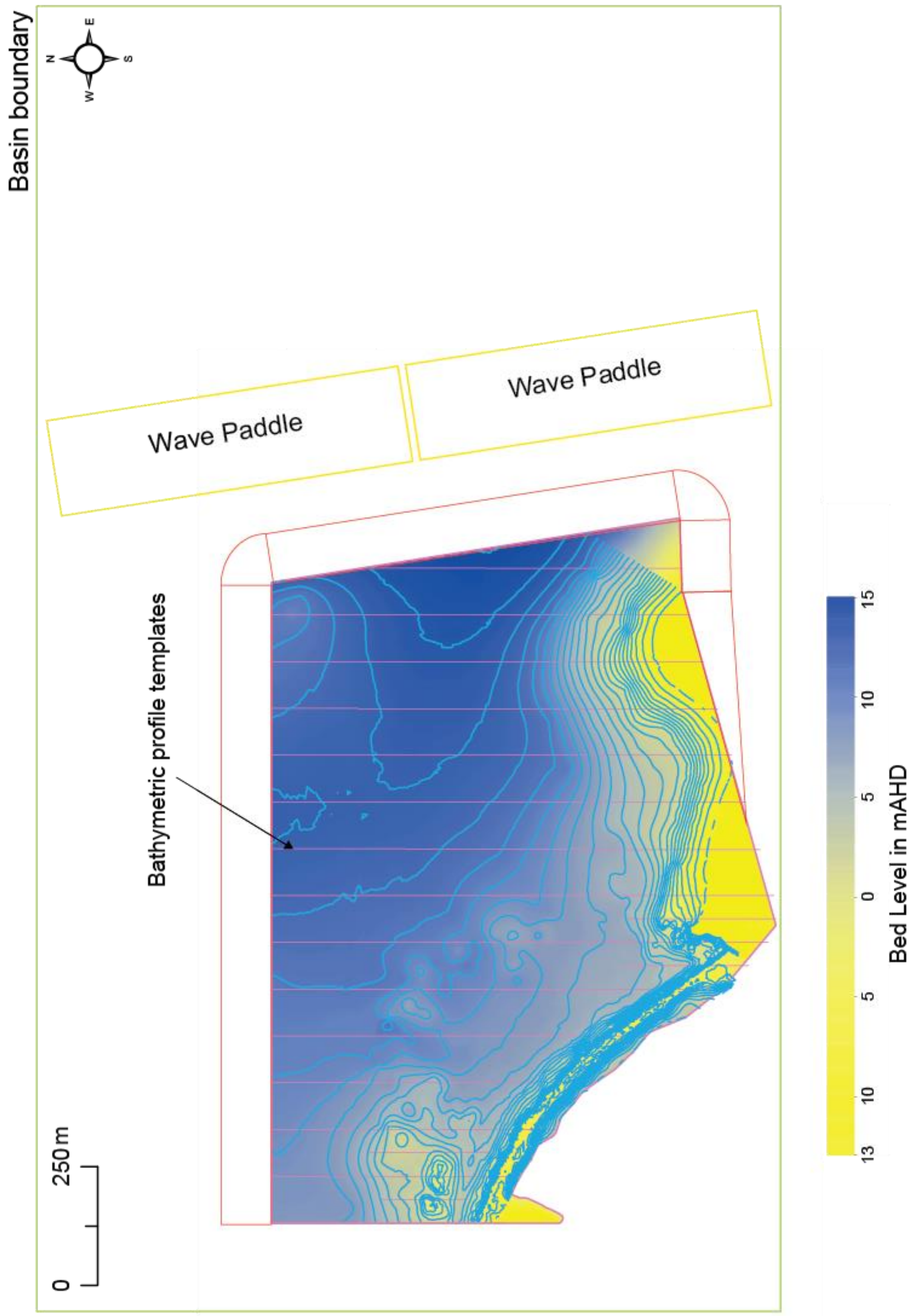

Figure 4.4: Wave Basin Layout

4.4.2 Bathymetry

Bathymetric details of the site were supplied to WRL by GHD as bathymetric data sets, and this information was used in the design and construction of the model bathymetry. Long sections through the bathymetry of the modelled area of the site were determined, and templates were produced that represented the bathymetric profile along these long sections. To best replicate the complexities of the sea bed and also expedite the model construction process, the templates were generally arranged at approximately 1 m spacing (model scale) aligned in a north-south direction. In areas of higher bathymetric complexity (such as around the Coffs Reef and Muttonbird Island), the spacing of the bathymetric templates was reduced to 0.5 m. This layout of bathymetric profile templates, as shown in Figure 4.4, provided adequate detail for the relatively complex bathymetry at the site.

Each bathymetry template was constructed from hardboard "Masonite", and was levelled into place using a laser line level, to an accuracy of ± 1.5 mm (model). The natural ocean floor areas were then constructed by infilling between the hardboard templates with recycled aggregate and capping with fibre reinforced concrete.

At the perimeter of the model bathymetry, the bathymetry was transitioned down to the wave basin floor at a slope of 1V:7H. The general guideline value (Hydralab, 2007) for this perimeter slope is 1V:10H. However, after significant consideration by WRL it was decided based on experience, that for this particular project the additional bathymetry gained by steepening the slope was more advantageous than sacrificing bathymetric extent for a flatter slope. This decision was primarily made to better understand the effect of the bathymetry on wave climate.

It was also decided to increase the roughness in the extended intertidal zone along Muttonbird Island after a preliminary round of testing, in order to introduce bottom friction and better represent wave behaviour in this area of the model.

4.4.3 Existing Breakwater Armour

The existing breakwater core material is largely impermeable, as such WRL constructed the core for the existing breakwater from aggregate fill overlain by a concrete capping. The surface of the core was covered with a glued layer of secondary armour rock in order to ensure realistic friction to the secondary and primary armour.

In the absence of available detailed data and on the basis of MHL (2004), the secondary rock armouring under/between the existing concrete cubes and below MSL was set as a widely graded material with mean rock size ~1 t (prototype scale).

A range of primary armour materials are present on the existing breakwater (8 t Hanbar units, 1 t rock and ~10 t concrete blocks). Existing model Hanbar units and concrete cubes were used for the testing, and with only one model length scale adopted, the selected scale was chosen to minimise the differences between the design mass for the 12 t and 20 t Hanbar units which were planned for the upgrade solutions. The Hanbar units were constructed from cast plastic with a representative density of 2300 kgm^{-3} (approximately equivalent to unreinforced concrete)and cubes from cement mortar with a representative density of 2100 kgm^{-3}. The difference between the design armour unit mass and that actually modelled is shown in Table 4.2.

Table 4.2: Primary Concrete Armour Specification for Existing Breakwater

Material	Origin	Design Armour Mass (t)	Equivalent Mass of Model Armour (t)
8 t Hanbar	Existing and New	8	8.0
Concrete Cube	Existing	10	7.2

It should be noted that the model concrete cube units used on the model are about 25% lighter, due to a lighter density material, than the concrete cubes currently placed on the Coffs Harbour northern breakwater. The most important factors when assessing overtopping are the shape (slope and elevation) of the breakwater and surface roughness (armour shape and approximate size) which were well reproduced in the breakwater model. It is believed that this mass difference did not have a great influence on the results modelling of the existing breakwater as this was performed only to validate overtopping against previous events and not armour stability.

4.4.4 Breakwater Upgrade Armour

Prior to placement of any new armour on the upgraded breakwater, removal of all concrete cubes and 8 t Hanbar units present on the existing breakwater was first undertaken, followed by a reshaping of the secondary 1 t rock armour to the provided elevation surveys.

- ***Rock Berm Armour***

Model armour for the rock berm in the breakwater upgrade were sorted, and gradings based on rock mass distribution were checked against those specified by GHD. Table 4.3 documents the various rock classes of primary and secondary armour rock used in the testing, with the grading curve for the upgrade berm rocks presented in Figure 4.5. Readily obtainable model rocks were sourced predominantly from Bass Point Quarry on the NSW south coast, the rock type being basalt with a representative density of approximately 2.65 t/m^3.

Table 4.3: Rock Armour Specifications

Armour Rock	Parameter	Design Values (kg)	Scaled Model Values (kg)[1]
Rock Berm 5-8 t	M_{MIN}		2,575
	M_{15}	5,000	4,450
	M_{50}	6,500	6,620
	M_{85}	8,000	8,220
	M_{MAX}		11,220
Existing Secondary (~1 T)	M_{MIN}		590
	M_{15}		785
	M_{50}	1,000	1,005
	M_{85}		1,348
	M_{MAX}		1,635

Note: (1) Model armour values are given at prototype scale to give an indication of potential differences when compared with the design values.

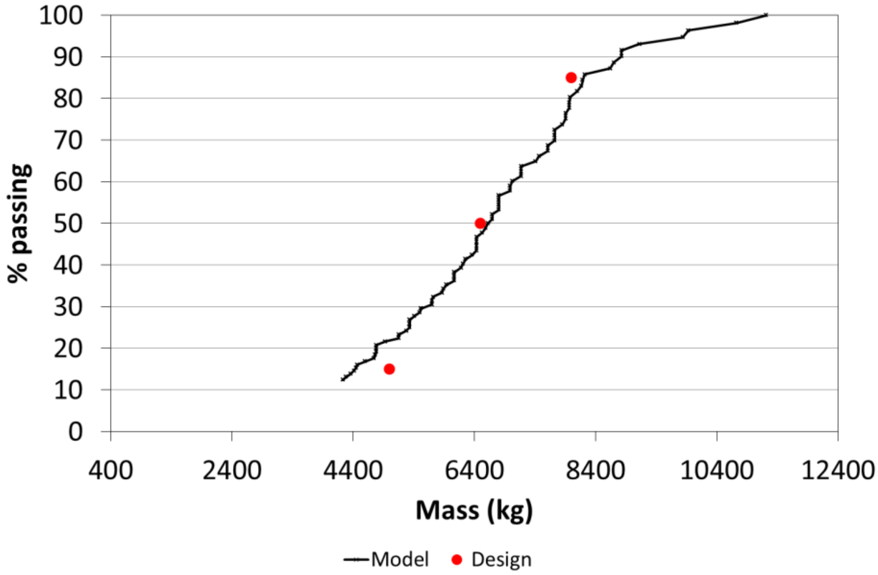

Figure 4.5: Grading curve for Upgrade Rock Berm armour

- ***Primary Armour***

A range of primary armour were used on the upgraded breakwater design, mainly 12 t and 20 t Hanbar units, with the addition of 5-8 tonne rock on both the eastern and western ends of the upgrades. Table 4.4 documents the different primary armour classes used in the testing for the breakwater upgrade designs.

The selected scale was chosen to minimise the differences between the design mass for the 12 t and 20 t Hanbar units and those used in the model. The Hanbar units were constructed from cast plastic with a representative density of 2300 kgm^{-3} (approximately equivalent to unreinforced concrete). The difference between the design armour unit mass and that actually modelled is shown in Table 4.4.

Table 4.4: Primary Concrete Armour Specification for Upgrade Designs

Material	Origin	Design Armour Mass (t)	Equivalent Mass of Model Armour (t)
12 t Hanbar	Existing and New	12	12.3
20 t Hanbar	Existing and New	20	19.6
Rock Armour	New	5 – 8	6.6 (M_{50})

4.5 Data Collection and Analysis

4.5.1 Wave Data

During each test, water surface elevation data was recorded at various locations by a series of six capacitance type wave probes. This data was logged at high frequency (200 Hz) using the National Instruments LabVIEW software package installed on a laboratory PC. Based on the time series of water surface elevations recorded by each wave probe, zero crossing and spectral analysis of the incident waves was able to be completed using the Mathworks MATLAB software package, which allowed calculation of the statistical wave distribution at each location.

Throughout the long duration (1000 waves minimum) irregular wave tests, incident waves from the wave generating paddles as well as reflected waves from the test structure continually pass one another throughout the wave basin. Both the incident and reflected waves are recorded in the water surface elevation records made by the capacitance wave probes. To be able to separate incident and reflected waves from a wave record, a least squares technique proposed by Mansard and Funke (1980), which utilises an array of three wave probes, was used. For this technique to be applied correctly, incident and reflected waves should be passing along the same line, but in opposite directions to one another. In this modelling study, one three probe array (3PA) was used to measure incident waves off the wave paddle, offshore of the breakwater location.

The three probe array was located at the -12.2 m AHD contour during all tests, and was setup so that the incident and reflected waves at the location of the probes were passing predominantly along the same alignment (it was not possible to have all reflected wave energy passing on the same alignment due to the irregular structure alignment). It was decided to use the three probe array technique at this location, which is equivalent to GHD SWAN modelling output Point 58, so that incident waves could be measured more accurately (without inclusion of reflected waves), and so that the actual incident wave height which was being generated could be estimated.

In addition to the three probe array deployed for all tests, three other individual wave probes were placed alongside the location of the breakwater in order to assess the changes in the wave climate due to wave processes such as refraction and reflection from the breakwater. The description, position and water depth of each wave probe is described in Table 4.5 and shown in Figure 4.6. Note that raw data records from probes $X1_{offshore}$, $X2_{offshore}$ and $X3_{offshore}$ are processed to form the 3PA statistics (with predominant wave reflections removed). The other wave probe records contain both incident and reflected wave energy, as indicated in this table.

Table 4.5: Summary of Wave Measurement Locations: Wave Climate Tests

Name	Description	GHD Swan Output Location	X (MGA 56)	Y (MGA 56)	Bed Level (m AHD)	Reflections?
3PA	Offshore Three Probe Array *	58	514464	6647764	-12.2	No
XO1	Seaward Probe in $3PA_1$	58	514464	6647764	-12.2	Yes
XO2	Centre Probe in $3PA_1$	~58	(variable)	(variable)	~-12.2	Yes
XO3	Landward Probe in $3PA_1$	~58	(variable)	(variable)	~-12.2	Yes
XB1	Southern Breakwater Probe	38	514126	6647683	-7.6	Yes
XB2	Centre Breakwater Probe	36	514223	6647593	-8.1	Yes
XB3	Northern Breakwater Probe	32	514264	6647542	-7.7	Yes

Note: (1) Raw data from probes $X1_{offshore}$, $X2_{offshore}$ and $X3_{offshore}$ are processed to form the 3PA statistics.

Zero up-crossing and zero down-crossing analyses were undertaken for each probe record after each test. The zero crossing analyses were used to determine the following wave statistics:

- T_Z mean wave period (s)
- T_p peak wave period (s)
- H_S average height of the highest 1/3rd of waves (m)
- H_{MAX} height of the single greatest wave height (m)

Note that for determining H_{MAX}, the single greatest wave height measured using the greater of the up-crossing and down-crossing assessments is reported (rather than an average of the two). Further to this, the peak wave period, T_P (s), was derived by spectral analysis corresponding to the peak spectral frequency, f_P; the frequency bin with the greatest amount of wave energy.

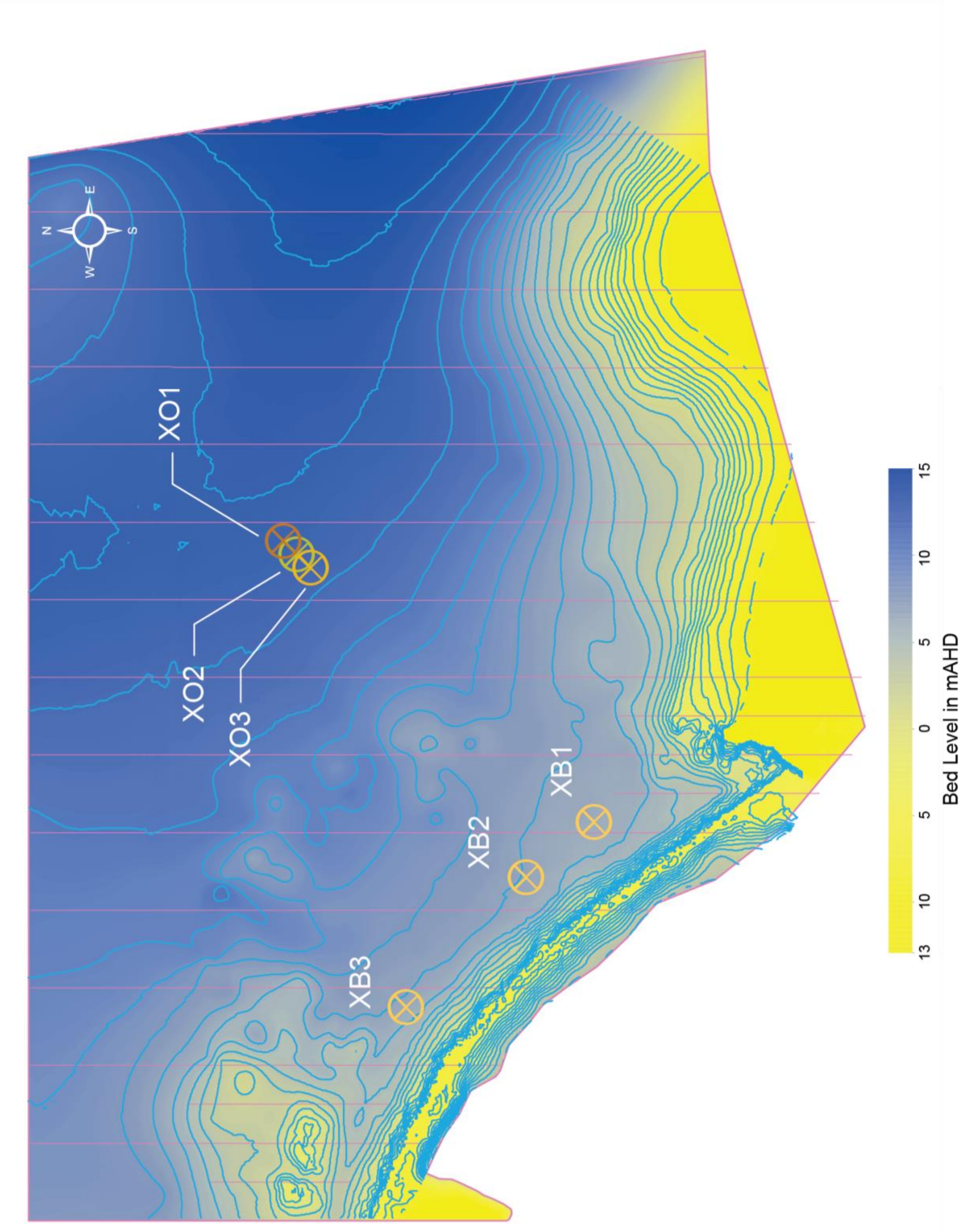

Figure 4.6: Wave Measurement Locations

4.5.2 Overtopping Data

Figure 4.7: Overtopping Measurement Locations

Average overtopping rates were measured using four (4) volumetric catch trays installed leeward of the breakwater crest, so that the total volume of overtopping water was captured and then averaged over the test duration. The 400 m long modelled section of the northern breakwater was therefore divided in four distinct 100 m long sections over which individual average overtopping rates were measured during testing. This allowed for more detailed understanding of the overtopping patterns and differences along the breakwater. The four overtopping catch trays were mounted flush with the crest of the breakwater such that it captured all overtopping flows, as shown on Figure 4.7.

If the volume of overtopping approached the capacity of the catch tray, the water in the catch tray was pumped into a separate receptacle, measured and tallied to give a cumulative overtopping volume for the test. This setup allowed the measurement of mean overtopping discharge, Q (L/s per m of crest length). Q was calculated by dividing the total volume of water that overtopped the structure, by the duration of the test (and then normalised to the length of breakwater crest).

4.5.3 Armour Layer Damage Assessment

Video footage (oblique) was recorded for each test, and used to support visual observations in assessment of armour damage. Still photographs of the armour (from an aerial position) were also taken of each breakwater structure prior to and following each armour stability test. A coloured banding system was used to aid in the tracking of individual primary armour units.

Armour damage classification was based on the guidelines presented in the Coastal Engineering Manual (USACE, 2006) and The Rock Manual (CIRIA; CUR; CETMEF, 2007). Damage was defined as units which were displaced from their original position by more than one equivalent cube diameter. The damage percentage was determined by relating the number of units displaced as a proportion of the total number of units in the complete primary armour layer or within a reference area. Additionally, given the large number of rocks used to build the rock berm, pre and post surveys of the berm were taken in order to supplement the visual assessment of damage observed during the tests.

5. Wave Climate Test Results

Each of the various test conditions (Table 3.1) were initially calibrated in the wave basin with the existing breakwater structure in place. Measured wave statistics for the calibrated test conditions are shown in Table 5.1 to Table 5.5. For each test, the target significant wave height was matched to within 0.2 m and the peak spectral wave period was also matched to within 0.6 s. Wave statistics reported for locations XO1, XO2, XO3, XB1, XB2 and XB3 include the effects of reflected waves within the basin. The data reported at location $3PA_{offshore}$ has had the effects of reflected waves removed by post processing analysis of the wave data from probes XO1, XO2, and XO3 using the method of Mansard and Funke (1980). Though the effects of reflected waves are small, the more reliable measurements at location $3PA_{offshore}$ were used to calibrate the wave timeseries. For subsequent armour stability and overtopping tests with the breakwater cross-sections in place, the respective wave climates presented in Table 5.1 to Table 5.5 were reproduced in the basin.

Table 5.1: Measured Wave Climate for 2004 Storm Event
(WL = 0.94 m AHD, H_s = 2.9 m, T_p = 12.5 s Target Test Conditions)

Name	Wave Period (s)		Wave Height (m)						Reflections?
	T_Z	T_P	H_{AVG}	H_{SIG}	$H_{10\%}$	$H_{5\%}$	$H_{1\%}$	H_{MAX}	
$3PA_{OFFSHORE}$	10.1	12.3	1.8	2.9	3.7	4.1	4.9	5.9	No
XO1	9.0	12.3	1.7	2.8	3.6	4.1	5.1	6.4	Yes
XO2	9.3	12.3	1.9	3.0	3.9	4.4	5.3	6.7	Yes
XO3	9.7	12.3	2.0	3.2	4.1	4.6	5.6	6.4	Yes
XB1	9.3	13.0	1.4	2.2	2.9	3.2	4.2	4.6	Yes
XB2	9.1	13.1	1.5	2.5	3.4	3.9	5.2	6.2	Yes
XB3	8.4	12.5	2.0	3.3	4.3	4.8	6.1	6.8	Yes

Table 5.2: Measured Wave Climate for 2009 Storm / 10 year ARI HAT Event
(WL = 1.20 m AHD, H_s = 4.8 m, T_p = 12.5 s Target Test Conditions)

Name	Wave Period (s)		Wave Height (m)						Reflections?
	T_Z	T_P	H_{AVG}	H_{SIG}	$H_{10\%}$	$H_{5\%}$	$H_{1\%}$	H_{MAX}	
$3PA_{OFFSHORE}$	9.9	12.6	3.0	4.7	5.8	6.2	7.0	7.5	No
XO1	9.0	12.3	3.0	5.0	6.3	7.0	8.1	8.8	Yes
XO2	9.4	12.5	3.3	5.3	6.6	7.2	8.1	8.8	Yes
XO3	9.4	12.8	3.3	5.4	6.9	7.6	8.6	9.4	Yes
XB1	7.7	13.5	2.3	3.9	4.9	5.4	6.2	6.6	Yes
XB2	7.5	12.9	3.0	5.3	6.7	7.5	9.4	10.1	Yes
XB3	8.2	12.4	3.0	5.0	6.2	6.7	7.5	8.0	Yes

Table 5.3: Measured Wave Climate for 100 year ARI HAT Event
(WL = 1.90 m AHD, H_s = 5.4 m, T_p = 15.3 s Target Test Conditions)

Name	Wave Period (s)		Wave Height (m)						Reflections?
	T_Z	T_P	H_{AVG}	H_{SIG}	$H_{10\%}$	$H_{5\%}$	$H_{1\%}$	H_{MAX}	
$3PA_{OFFSHORE}$	10.5	15.1	3.4	5.4	6.4	6.8	7.5	7.9	No
XO1	10.1	15.1	3.6	5.9	7.7	8.4	9.6	10.8	Yes
XO2	10.3	15.1	3.8	6.2	7.9	8.6	10.0	11.4	Yes
XO3	10.4	15.1	3.8	6.2	7.9	8.6	9.9	11.2	Yes
XB1	7.6	15.3	2.0	3.4	4.4	4.9	5.9	6.7	Yes
XB2	8.0	15.0	2.9	5.1	6.9	7.7	9.7	12.9	Yes
XB3	7.6	14.8	2.9	5.0	6.1	6.5	7.3	7.5	Yes

Table 5.4: Measured Wave Climate for 100 year ARI HAT+SLR Event
(WL = 1.20 m AHD, H_s = 5.5 m, T_p = 15.3 s Target Test Conditions)

Name	Wave Period (s)		Wave Height (m)						Reflections?
	T_Z	T_P	H_{AVG}	H_{SIG}	$H_{10\%}$	$H_{5\%}$	$H_{1\%}$	H_{MAX}	
$3PA_{OFFSHORE}$	10.5	15.1	3.5	5.5	6.7	7.1	7.7	8.0	No
XO1	10.0	15.1	3.6	6.0	7.7	8.4	9.7	10.2	Yes
XO2	10.2	15.1	3.8	6.3	8.2	9.0	10.4	11.5	Yes
XO3	10.1	15.1	3.8	6.4	8.1	8.8	10.2	11.3	Yes
XB1	8.1	15.1	2.1	3.6	4.6	5.1	6.0	6.9	Yes
XB2	8.1	15.1	2.9	5.1	6.9	7.7	9.2	10.1	Yes
XB3	7.9	15.1	3.0	5.2	6.4	7.0	8.4	9.2	Yes

Table 5.5: Measured Wave Climate for 100 year ARI MSL Event
(WL = 0.0 m AHD, Uncalibrated H_s and T_p Test Conditions)

Name	Wave Period (s)		Wave Height (m)						Reflections?
	T_Z	T_P	H_{AVG}	H_{SIG}	$H_{10\%}$	$H_{5\%}$	$H_{1\%}$	H_{MAX}	
$3PA_{OFFSHORE}$	10.3	14.7	3.1	4.8	5.7	6.1	6.7	7.1	No
XO1	10.2	14.8	3.3	5.4	6.9	7.5	8.9	10.0	Yes
XO2	10.4	14.6	3.4	5.7	7.1	7.7	9.3	10.1	Yes
XO3	10.6	14.5	3.4	5.7	7.0	7.6	8.5	9.0	Yes
XB1	8.8	15.4	2.1	3.6	4.5	4.9	5.5	6.1	Yes
XB2	9.1	14.5	2.6	4.4	5.3	5.7	6.6	7.5	Yes
XB3	8.4	12.7	2.6	4.4	5.4	5.7	6.5	7.0	Yes

6. Model Validation - Historical Storm Event Testing

6.1 Introduction

Testing of the existing northern breakwater was first undertaken in order to validate the physical model. Model validation testing involved a qualitative assessment of the overtopping processes along the existing breakwater for several storm events that have previously occurred. After discussion with GHD and Crown Lands, it was agreed to perform the historical validation for the following storm events:

- 6th March 2004; and
- 22nd May 2009.

Significant overtopping was observed and photographed at several locations along the breakwater during both of these events. Furthermore, analysis of the events had previously been completed by Watterson and Driscoll (2011).

6.2 Model Construction Details

A model of the current northern breakwater was constructed from chainage 400 m to 840 m based on all available information, which consisted of:

- Cross section surveys of the existing breakwater (50 m spacings) from 2007;
- Aerial photographs of the breakwater from Sixmaps;
- Videos from boat survey traverse along the structure; and
- Information and photos in the MHL Breakwater Asset Appraisal and Physical Model report (MHL, 2004).

On the basis of the information from these sources, WRL was able to get an understanding of the armouring along the seaward face of the breakwater located above MSL and establish the following approximate armour breakdown:

Table 6.1: Breakdown of Primary Concrete Armour Observed on Existing Breakwater

Chainage	Estimated Number of 10 t Concrete Cubes	Estimated Number of 8 T Hanbars
400-460	79	0
460-510	97	0
510-575	79	35
575-630	57	49
630-690	94	0
690-730	52	0
730-800	39	0
Total	**497**	**84**

a) Overview of Existing Breakwater Core with Templates

b) Overview of Existing Breakwater Armoured with Concrete Cubes and Hanbars

Figure 6.1: Existing Breakwater Construction

It should be noted that the modelling of the existing breakwater was primarily performed to validate the main wave processes in the model and qualitatively verify the overtopping processes experienced during previous events. In particular, attention was given to accurately reproduce the shape (slope and elevation) of the armoured breakwater by using templates derived from the most recent breakwater cross section survey (available every 50 m of chainage); as well as the surface roughness (armour shape and approximate size).

6.3 2004 Historical Event

The first test performed for the historical validation component of the project aimed to reproduce the 6th March 2004 storm event. This event had a duration of approximately 24 hours (with H_s> 3 m), predominant swell direction from the east to northeast, and a peak H_s of 4.0 m (Watterson and Driscoll, 2011). It was reported that this storm resulted in medium overtopping hazard condition at the breakwater crest, with white-water overtopping reaching up to 3 to 4 m above the crest and a small amount of green-water overtopping the structure. WRL was provided with a set photographs taken from the crest of the breakwater during the storm in order to perform a qualitative comparison with the overtopping processes observed in the model. Further analysis of these pictures (Figure 6.2) showed that most of the overtopping consisted of large spray (white water) over the breakwater crest between chainage 500 m and 700 m, which can be seen to have reached heights of up to 6 m.

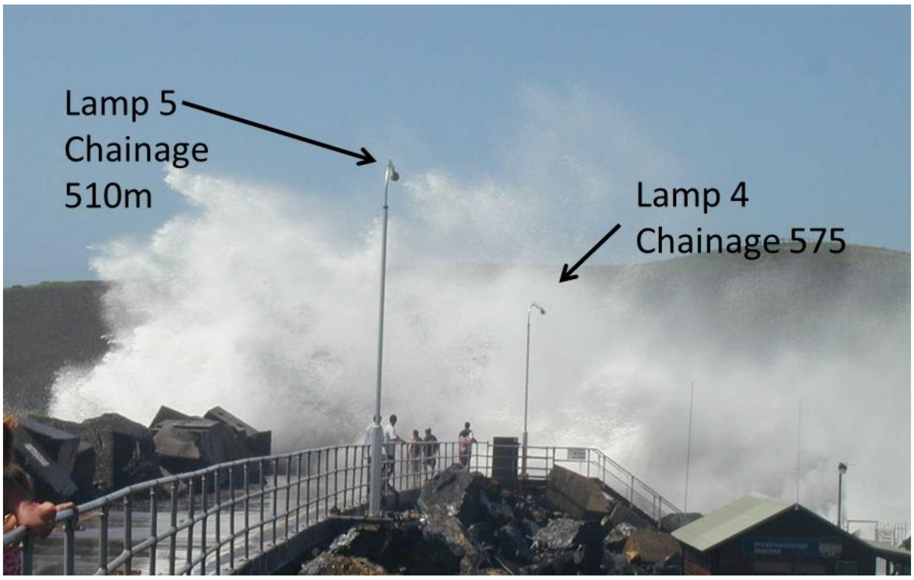

a) Overtopping Spray from Ch. 600 m to Ch. 700 m

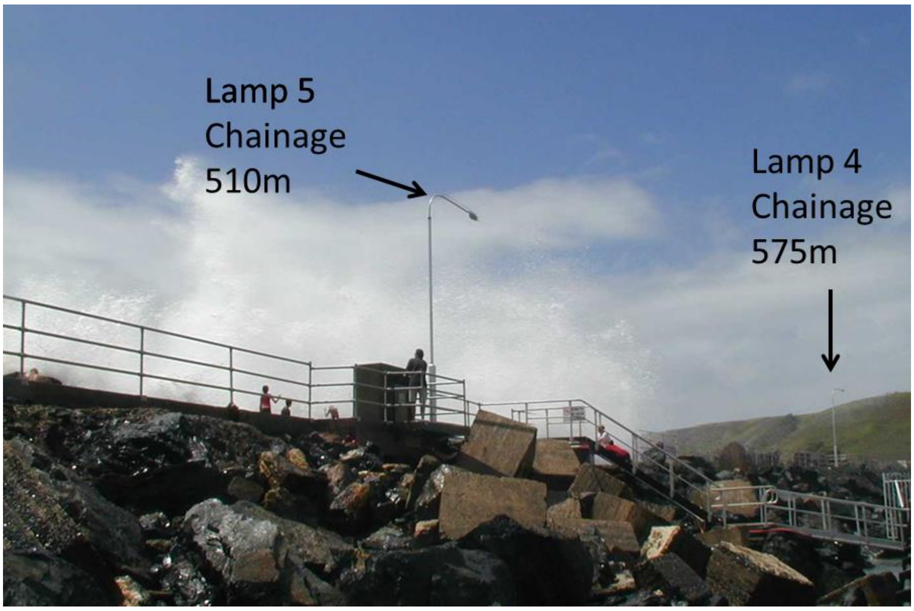

b) Example of Vertical Overtopping Spray around Ch. 550 m

Figure 6.2: Observed Wave Overtopping Conditions during the 2004 Event

The peak wave/water level conditions for the March 2004 storm event were reproduced in the physical model, with observations of the overtopping recorded. Observed overtopping in the model mainly consisted in vertical spray over the crest across overtopping trays OT 2 (ch. 500 m – ch. 600 m) and OT 3 (ch. 600 m – ch. 700 m). On a very limited number of instances (less than 10 occurrences over a 2 hour prototype scale test duration), large breaking waves were observed to result in a small amounts of green water being projected in the overtopping catch trays, predominantly around ch. 600 m. Very limited overtopping of the structure could be observed across catch trays OT 1 (ch. 400 m – ch. 500 m) and OT 4 (ch. 700 m – ch. 800 m), and consisted only of vertical spray, due to the absence of wind in the modelling.

a) Overtopping Spray from Ch. 575 m to Ch. 625 m

b) Example of Overtopping around Ch. 550 m

Figure 6.3: Observed Wave Overtopping Conditions for the 2004 Event Model Test

The qualitative overtopping observations in the physical model test were considered to be relatively consistent with the photographs taken of the real world breakwater during the storm event. The quantitative results of overtopping assessment for the 2004 historical event are illustrated in Table 6.2. Based on the published tolerable rates (USACE, 2006; EurOtop, 2007), the measured average overtopping rates during this test would be classified as a potential hazard to pedestrians but not to the structure, which is also considered to be consistent with the level of overtopping observed at the site during the storm event.

Table 6.2: Overtopping Results for 2004 Event (Prototype Scale)

Event	Peak Water Level (m AHD)	Peak H_s (m)	T_p (s)	Chainage (m)	Ave. Overtopping Rate (L/s/m)
March 2004	0.94	2.9	12.5	400-500	0.00
				500-600	1.26
				600-700	0.93
				700-800	0.00

6.4 2009 Historical Event

The second test performed for the historical validation component of the project aimed to reproduce the 22nd May 2009 storm event. This event was considerably more powerful than the 2004 event. The storm lasted over 96 hours (with H_s> 3 m), had a predominant swell direction from the east, and a peak H_s of 6.5 m (Watterson and Driscoll, 2011). This storm was reported to have caused significant structural damage to the crest of the breakwater, and to have resulted in medium overtopping hazard conditions at the breakwater crest, with several 10 t concrete cubes being carried into the marina by overtopping wave bores. WRL was provided with multiple sets of photographs from different viewpoints (Figure 6.4, Figure 6.5 and Figure 6.6) taken during the storm, which were used to undertake a comparison with the overtopping processes observed in the model.

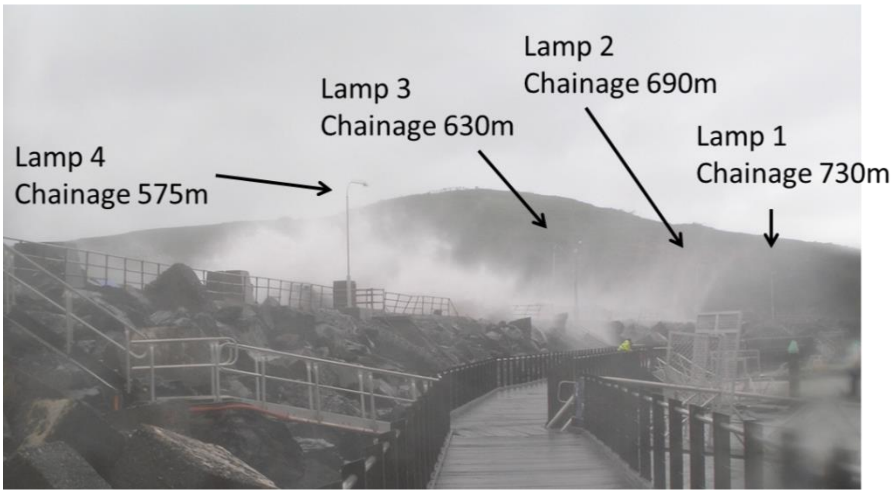

a) Overtopping Spray from Ch. 575 m to Ch. 700 m

b) Example of Green-Water Overtopping around Ch. 600 m

Figure 6.4: Observed Wave Overtopping Conditions for the 2009 Event

Figure 6.5: Observed Wave Overtopping and Resulting Damage from Surveillance Camera

Figure 6.6: Observed Wave Overtopping from Muttonbird Island

As expected, the observed overtopping during model testing was significantly larger and more frequent than observed for the 2004 test event. As an indication, the breakwater crest along overtopping catch tray OT 2 (ch. 500 m – ch. 600 m) was overtopped nearly 200 times while OT 4 (ch. 700 m – ch. 800 m) was overtopped more than 50 times during the two hour (prototype scale) duration of the test. Overtopping in the model could mostly be characterised as green-water, with several stretches of breakwater crest submerged simultaneously (about 100 m stretches).

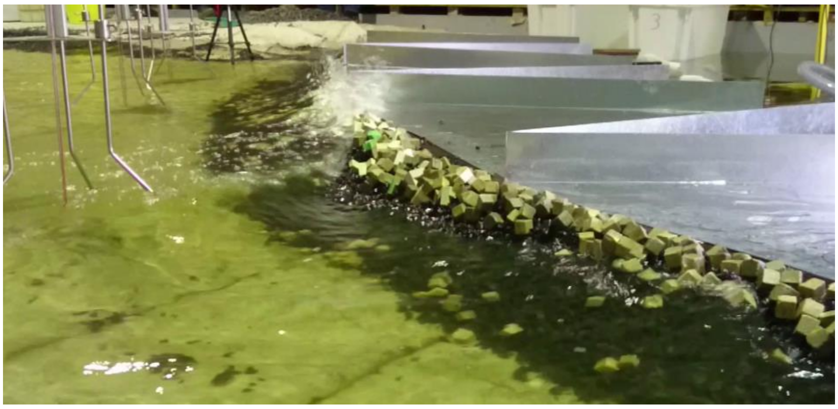

a) Simultaneous Green-Water Overtopping from Ch. 550 m to Ch. 600 m

b) Large Overtopping Sequence from Ch. 575 m to Ch. 700 m

c) Overtopping Sequence from Ch. 650 m to Ch. 750 m with Displaced Concrete Cubes

Figure 6.7: Observed Wave Overtopping Conditions for the 2009 Event Model Test

Approximately 12 concrete cubes as well as secondary armour rocks were observed to be displaced by overtopping wave bores and carried over the crest of the breakwater. It can be seen from the overtopping assessment results provided in Table 6.3 that the breakwater was significantly overtopped throughout the duration of the test. The central and southern sections (i.e. ch. 500 m to ch. 800 m) were subject to average overtopping rates that largely exceeded what would be classified as a hazard to pedestrians (>10 L/s/m), with the section around ch. 650 m reaching values typically associated with potential structural damage to the structure itself and sinking yachts located in the lee of the breakwater.

Table 6.3: Overtopping Results for 2009 Event (Prototype Scale)

ARI Event	Water Level (m AHD)	H_s (m)	T_p (s)	Chainage (m)	Ave. Overtopping Rate (L/s/m)
2009	1.2	4.8	12.5	400-500	2.64
				500-600	13.22
				600-700	60.93
				700-800	10.47

Both the quantitative overtopping values as well as the qualitative observations made during model run of the 2009 storm event, were consistent with the observations from the real world event.

7. Armour Stability Test Results

7.1 Introduction

Primary armour, crest specific armour units as well as rock berm stability for the proposed upgraded breakwater design was investigated under 10 year ARI and 100 year ARI wave conditions. The results for each of the tested upgrade designs (Upgrade 8a and Upgrade 8b) are presented in the following report sections and illustrated by still photographs prior to and following each armour stability test.

The tests were undertaken in a cumulative manner (no rebuild of the breakwater armour layer in between tests) in the following sequence order for Upgrade 8:

- 10 year ARI HAT event (WL = 1.20 m AHD, H_s = 4.8 m, T_p = 12.5 s);
- 100 year ARI HAT SLR (WL = 1.90 m AHD, H_s = 5.5 m, T_p = 15.3 s); and
- 100 year ARI MSL (WL = 0.00 m AHD, H_s = 4.8 m, T_p = 14.7 s).

The tests were undertaken in a cumulative manner (no rebuild of the breakwater armour layer in between tests) in the following sequence order for Upgrade 8b:

- 10 year ARI HAT event (WL = 1.20 m AHD, H_s = 4.8 m, T_p = 12.5 s); and
- 100 year ARI HAT SLR (WL = 1.90 m AHD, H_s = 5.5 m, T_p = 15.3 s).

7.2 Breakwater Upgrade 8a Testing

7.2.1 Upgrade 8a Design

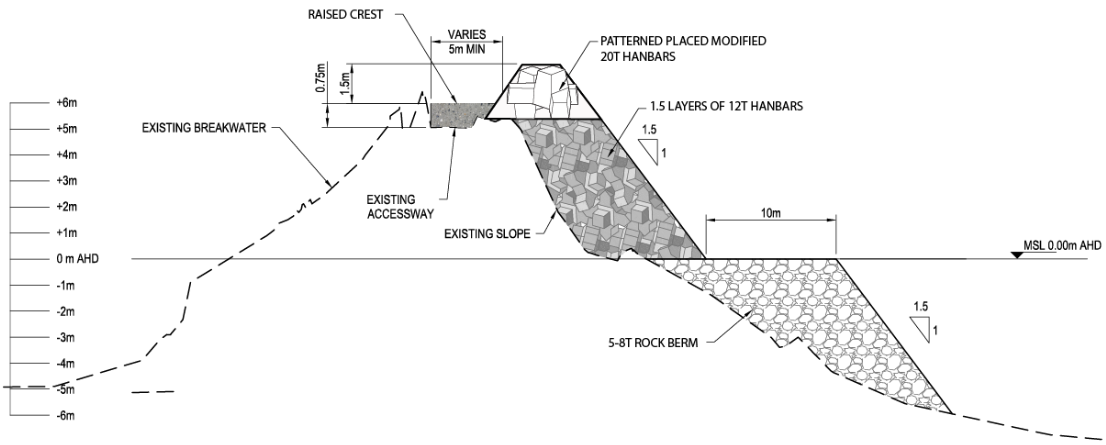

Figure 7.1: Upgrade 8a Design (Concept Only – Not for Construction)

Figure 7.1 shows the design of Upgrade 8a as tested. Prior to placement of any new armour on the breakwater, removal of all concrete cubes present on the existing breakwater was first undertaken, followed by a reshaping of the secondary 1 t rock armour to the provided elevation surveys. The existing access way on the breakwater crest was raised by 0.75 m and widened to provide a minimum width of 5 m. Upgrade 8a was built with a 10 m wide rock berm at MSL constructed from 5-8 tonne rock with 1V:1.5H front slope. Above MSL Upgrade 8a was built with a primary armour layer consisting of 12 t Hanbar units placed on the existing structure to an overall density of 31 units per 100 m^2, amounting to a total of 1087 units over the whole model. The 12 t Hanbar units were placed with a ratio of 60:40 for bottom:top layer. The crest of Upgrade 8a consisted of a total of 136 patterned placed modified 20 t Hanbar units. These "crest containment" units were developed by reducing the vertical arm of 20 t Hanbar units to achieve a reduced overall height of 2.3 m. This patterned placed crest armour resulted in an effective overall unit crest height 1.5 m higher than the accessway level. A detail view of the built crest with the pattern placed modified 20 t Hanbar units is provided in Figure 7.2.

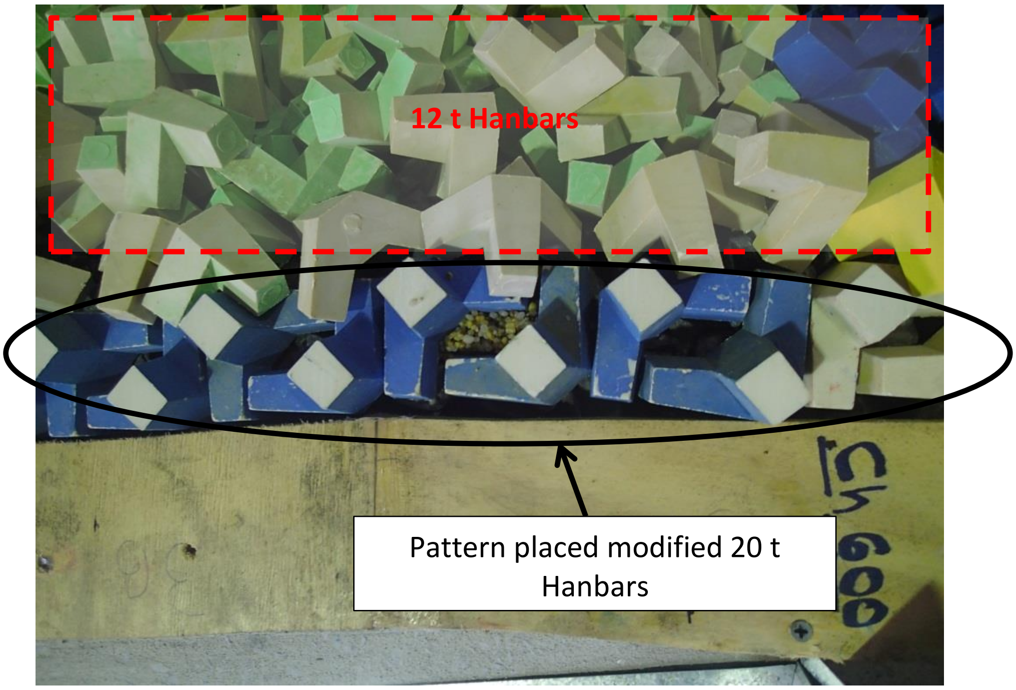

Figure 7.2: Detail View (Plan) of Upgrade 8a crest

A brief summary of the nature and extent of the observed damage during each of the consecutive armour stability tests is presented in Sections 7.2.2 to 7.2.4. The cumulative damage to the primary armour, crest containment units and rock toe berm is presented in Table 7.1 for each armour stability test. Photographs of the model "as built" and after each tests are presented in Figure 7.3, Figure 7.4 and Figure 7.5. 2D laser profiles of the model breakwater "as built" and after each test are presented in Appendix A in order to provide additional information on the evolution of the rock berm.

7.2.2 10 year ARI HAT Armour Stability Test

For the 10 year ARI event with a 1.2 m AHD water level (HAT), only small persistent rocking motions for less than 2% of the 12 t Hanbars on seaward slope were observed. A total of four 12 t Hanbar units were observed to be displaced and move down the front face onto the rock berm, amounting for 0.4% of the total number of 12 t units. No rocking or displacement of the modified 20 t Hanbars located near the crest was observed throughout the test. There was also negligible damage to the 5-8 tonne rock berm, with the majority of the displaced rocks coming from the upper part of the front slope.

7.2.3 100 year ARI HAT+ SLR Armour Stability Test

For the 100 year ARI event with a 1.9 m AHD water level (HAT + SLR), small to violent persistent rocking motions for less than 2% of the 12 t Hanbars on seaward slope were again observed. A total of six of the 12 t Hanbar units were observed to be displaced and move down the front face onto and across the rock berm, amounting for 0.6% of the total number of 12 t units. No rocking or displacement of the modified 20 t Hanbars located near the crest was observed throughout the test. While damage to the 5-8 tonne rock berm could still be considered negligible, some of the 5-8 tonne rocks located on the flat part of the berm were observed to violently rock back and forth, impacting the lower rows of 12 t Hanbar units.

Very small diameter gravel was inserted between the crest containment units located near the crest of the breakwater before the test in order to qualitatively investigate the risk of fill material being carried over the access way and into the marina during large storm events. This small diameter material was observed to be carried behind the crest of the structure during the largest overtopping events. Waves were observed to run predominantly transversely across the 12 t Hanbar slope between ch. 425 m to ch. 500 m, with some jetting between the Hanbar to rock slope transition, which could cause an increase risk to the rock armour stability.

7.2.4 100 year ARI MSL Armour Stability Test

For the 100 year ARI event with a 0.0 m AHD water level (MSL), small to violent persistent rocking motions for less than 1% of the 12 t Hanbars on seaward slope were again observed, exclusively on the lower rows of the slope. Cumulative overall damage increased up to 0.7% of the 12 t Hanbar units, with a total of 8 units displaced from their initial position. No rocking or displacement of the modified 20 t Hanbars located near the crest was observed throughout the test. The overall amount of the damage to the rock berm could still be considered minimal but extended along nearly the whole length of the breakwater. Again, some berm rocks were observed to be violently rocking back and forth, impacting some of the lower 12 t Hanbar units.

Table 7.1: Summary of Upgrade 8a Armour Stability Tests

Chainage (m)	Armour Type and Location	Colour Band	Armour Size (t)	Number of Units Placed	Test Event					
					10 year ARI HAT		100 year ARI HAT SLR		100 year ARI MSL	
					Number of Units Damaged[1]	Damage[1] (%)	Number of Units Damaged[1]	Damage[1] (%)	Number of Units Damaged[1]	Damage[1] (%)
425-475	Rock Berm	White/Yellow	6.5	-	5	N.A.	8	N.A.	12	N.A.
	Rock Slope	Blue	6.5	-	7	N.A.	10	N.A.	12	N.A.
	Rock Crest	White	6.5	-	0	N.A.	0	N.A.	0	N.A.
475-500	Rock Berm	Pink	6.5	-	6	N.A.	11	N.A.	15	N.A.
	Hanbar Slope	White/Yellow	12	71	0	0.0%	0	0.0%	0	0.0%
	Hanbar Crest	Blue	19	11	0	0.0%	0	0.0%	0	0.0%
500-550	Rock Berm	Blue/White/Yellow	6.5	-	7	N.A.	15	N.A.	22	N.A.
	Hanbar Slope	Pink/Yellow	12	173	0	0.0%	1	0.6%	1	0.6%
	Hanbar Crest	White	19	22	0	0.0%	0	0.0%	0	0.0%
550-600	Rock Berm	Blue/White/Yellow	6.5	-	3	N.A.	5	N.A.	8	N.A.
	Hanbar Slope	Green/White	12	196	1	0.5%	1	0.5%	2	1.0%
	Hanbar Crest	Blue	19	22	0	0.0%	0	0.0%	0	0.0%
600-650	Rock Berm	Blue/White/Yellow	6.5	-	6	N.A.	8	N.A.	9	N.A.
	Hanbar Slope	Blue/Yellow	12	201	1	0.5%	1	0.5%	1	0.5%
	Hanbar Crest	White	19	22	0	0.0%	0	0.0%	0	0.0%
650-700	Rock Berm	Blue/White/Yellow	6.5	-	2	N.A.	3	N.A.	7	N.A.
	Hanbar Slope	Green/White	12	183	1	0.5%	2	1.1%	3	1.6%
	Hanbar Crest	Blue	19	24	0	0.0%	0	0.0%	0	0.0%
700-750	Rock Berm	Blue/White/Yellow	6.5	-	2	N.A.	2	N.A.	4	N.A.
	Hanbar Slope	White/Yellow	12	172	0	0.0%	0	0.0%	0	0.0%
	Hanbar Crest	White	19	22	0	0.0%	0	0.0%	0	0.0%
750-775	Rock Berm	Pink/White/Yellow	6.5	-	0	N.A.	1	N.A.	0	N.A.
	Hanbar Slope	Green/White/Yellow	12	91	1	1.1%	1	1.1%	1	1.1%
	Hanbar Crest	Blue	19	13	0	0.0%	0	0.0%	0	0.0%

[1] Note that the damage recorded is a cumulative damage and represents the incremental damage during the given test sequence.

Chainage (m)	"As-Built"	After 10 year ARI HAT	After 100 year ARI HAT SLR	After 100 year ARI MSL
425-475				
475-500				
500-550				

Figure 7.3: Upgrade 8a Cumulative Damage Assessment (1/3)

Chainage (m)	"As-Built"	After 10 year ARI HAT	After 100 year ARI HAT SLR	After 100 year ARI MSL
550-600				
600-650				
650-700		 		

Figure 7.4: Upgrade 8a Cumulative Damage Assessment (2/3)

Chainage (m)	"As-Built"	After 10 year ARI HAT	After 100 year ARI HAT SLR	After 100 year ARI MSL
700-750				
750-800				

Figure 7.5: Upgrade 8a Cumulative Damage Assessment (3/3)

7.3 Breakwater Upgrade 8b Testing

7.3.1 Upgrade 8b Design

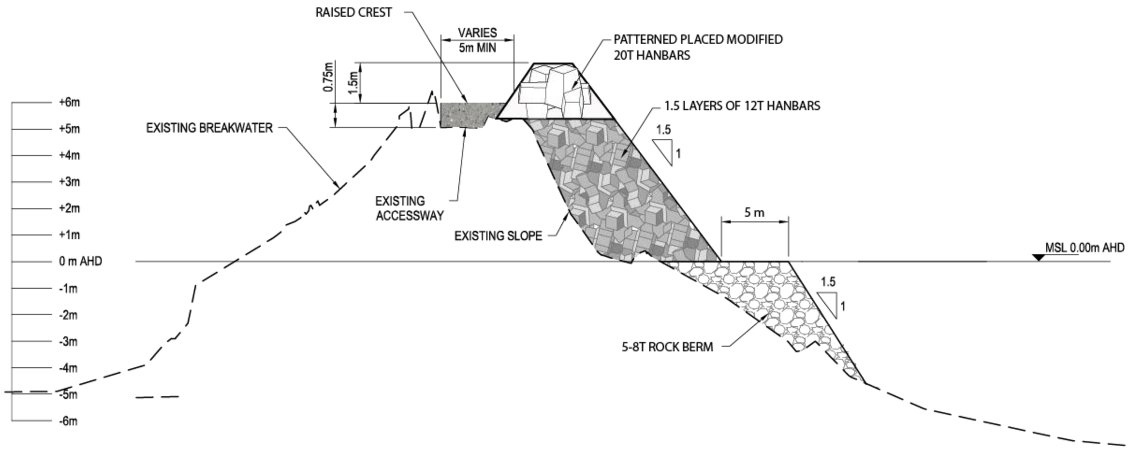

Figure 7.6: Upgrade 8b Design (Concept Only – Not for Construction)

Figure 7.6 shows the design of Upgrade 8b as tested. The only change to the structure design, compared to the design of Upgrade 8, is a reduction of the flat section of the rock berm to a width of 5 m. The structure was rebuilt using the exact same combination and number of 12 t Hanbar units placed on the seaward slope to an overall density of 31 units per 100 m^2. The crest of Upgrade 8b was also constructed identical to the crest of Upgrade 8.

A brief summary of the nature and extent of the observed damage during each of the consecutive armour stability tests is presented in Sections 7.3.2 and 7.3.3. The cumulative damage to the primary armour, crest containment units and reduced rock toe berm is presented in Table 7.2 for each armour stability test. Photographs of the model "as built" and after each test are presented in Figure 7.7, Figure 7.8 and Figure 7.9. 2D laser profiles of the model "as built" and after each test are presented in Appendix B in order to provide additional information on the evolution of the rock berm.

7.3.2 10 year ARI HAT Stability Test

For the 10 year ARI event with a 1.2 m AHD water level (HAT), only small persistent rocking motions for 1% of the 12 t Hanbars on seaward slope were observed. A total of six 12 t Hanbar units were observed to be displaced and moved down the front face onto the rock berm. This is more than the four 12 t Hanbar units displaced for Option 8a and amounts to 0.6% of the total number of 12 t Hanbar units. No rocking or displacement of the modified 20 t Hanbars located near the crest could be observed throughout the test. While damage to the reduced 5-8 tonne rock berm could still be considered negligible, waves were observed to be more frequently breaking directly on the two lower rows of 12 t Hanbar units. Damage to the rock berm was observed to occur more readily, and was thought to be the result of more of a sucking action of the waves breaking on the rock armour over the flat part of the berm, compared to Option 8.

7.3.3 100 year ARI HAT+ SLR Stability Test

For the 100 year ARI event with a 1.9 m AHD water level (HAT + SLR), small to violent persistent rocking motions for 1% of the 12 t Hanbars on seaward slope were again observed. A total of nine 12 t Hanbar units were observed to be displaced and moved down the front face onto and across the rock berm. This is more than the six 12 t Hanbar units displaced for Option 8a and amounts to 0.8% of the total number of 12 t Hanbar units. No rocking or displacement of the modified 20 t Hanbars located near the crest was observed during the test. While damage to the 5-8 tonne rock berm could still be considered negligible, some of the 5-8 tonne rocks located on the flat part of the berm were observed to violently rock back and forth, impacting the lower rows of 12 t Hanbar units.

Waves were again observed to run predominantly transversely across the 12 t Hanbar slope between ch. 425 m to ch. 500 m, with some jetting between the Hanbar to rock slope transition, which could cause an increase risk to the rock armour stability. It should be noted that during a large overtopping event, one 3.2 t rock (prototype scale) was dislodged from the rock crest around ch. 450 m and carried leeward of the crest access way. It should be noted that the mass of this displaced rock is below the M_{15} of the rock mass distribution used for the 5-8 tonne rock berm.

Table 7.2: Summary of Upgrade 8b Armour Stability Tests

Chainage (m)	Armour Type and Location	Colour Band	Armour Size (t)	Number of Units Placed	Test Event: 10 year ARI HAT – Number of Units Damaged[1]	Test Event: 10 year ARI HAT – Damage[1] (%)	Test Event: 100 year ARI HAT SLR – Number of Units Damaged[1]	Test Event: 100 year ARI HAT SLR – Damage[1] (%)
425-475	Rock Berm	White/Yellow	6.5	-	6	N.A.	7	N.A.
	Rock Slope	Blue	6.5	-	5	N.A.	5	N.A.
	Rock Crest	White	6.5	-	0	N.A.	1	N.A.
475-500	Rock Berm	Pink	6.5	-	8	N.A.	10	N.A.
	Hanbar Slope	White/Yellow	12	71	0	0.0%	0	0.0%
	Hanbar Crest	Blue	19	11	0	0.0%	0	0.0%
500-550	Rock Berm	Blue/White/Yellow	6.5	-	6	N.A.	0	N.A.
	Hanbar Slope	Pink/Yellow	12	173	2	1.2%	3	1.7%
	Hanbar Crest	White	19	22	0	0.0%	0	0.0%
550-600	Rock Berm	Blue/White/Yellow	6.5	-	15	N.A.	17	N.A.
	Hanbar Slope	Green/White	12	196	0	0.0%	1	0.5%
	Hanbar Crest	Blue	19	22	0	0.0%	0	0.0%
600-650	Rock Berm	Blue/White/Yellow	6.5	-	9	N.A.	12	N.A.
	Hanbar Slope	Blue/Yellow	12	201	2	1.0%	2	1.0%
	Hanbar Crest	White	19	22	0	0.0%	0	0.0%
650-700	Rock Berm	Blue/White/Yellow	6.5	-	1	N.A.	4	N.A.
	Hanbar Slope	Green/White	12	183	1	0.5%	2	1.1%
	Hanbar Crest	Blue	19	24	0	0.0%	0	0.0%
700-750	Rock Berm	Blue/White/Yellow	6.5	-	4	N.A.	5	N.A.
	Hanbar Slope	White/Yellow	12	172	1	0.6%	1	0.6%
	Hanbar Crest	White	19	22	0	0.0%	0	0.0%
750-775	Rock Berm	Pink/White/Yellow	6.5	-	0	N.A.	1	N.A.
	Hanbar Slope	Green/White/Yellow	12	91	0	0.0%	0	0.0%
	Hanbar Crest	Blue	19	13	0	0.0%	0	0.0%

[1] Note that the damage recorded is a cumulative damage and represents the incremental damage during the given test sequence.

Chainage (m)	"As-built"	After 10 year ARI HAT	After 100 year ARI HAT SLR
425-475			
475-500			
500-550			

Figure 7.7: Upgrade 8b Cumulative Damage Assessment (1/3)

Chainage (m)	“As-built”	After 10 year ARI HAT	After 100 year ARI HAT SLR
550-600			
600-650			
650-700			

Figure 7.8: Upgrade 8b Cumulative Damage Assessment (2/3)

Chainage (m)	"As-built"	After 10 year ARI HAT	After 100 year ARI HAT SLR
700-750			
750-800			

Figure 7.9: Upgrade 8b Cumulative Damage Assessment (3/3)

8. Overtopping Test Results

8.1 Introduction

Overtopping tests were performed for the two different breakwater upgrade designs:

- Upgrade 8a (with a 10 m wide rock berm); and
- Upgrade 8b (with a 5 m wide rock berm).

As discussed in Section 4.5.2, assessment of overtopping of the breakwater was discretised into 100 m long (prototype scale) adjacent sections in order to provide information regarding the distribution of overtopping, and to assist in identifying higher risk sections of the structure.

During storm events, wave overtopping of the breakwater crest is likely to occur in the form of green-water wave bores flowing over the crest into the marina, or white-water spray of water being projected upwards and eventually transported on and over the crest by onshore winds. Wave overtopping can cause serious structural damage to the breakwater crest and to infrastructure immediately behind the breakwater. Overtopping also constitutes a direct hazard to pedestrians and vehicles on the breakwater crest during storm events.

Wave overtopping is measured as the volume of water discharged over the breakwater crest level averaged over the duration of the test, and expressed as an average rate in *L/s per m.* The estimated overtopping rates refer to the zone immediately behind the structure crest and can be related to the published tolerable rates (USACE, 2006; EurOtop, 2007) with regard to structural damage and safety of people. The tolerable overtopping rates presented in EurOtop (2007) are considered among industry as the best available guideline and are reproduced in Table 8.1.

Table 8.1: Limits for Tolerable Mean Wave Overtopping Discharges (EurOtop 2007)

Hazard type	**Mean Overtopping Discharge Limit** (L/s per m)
Aware **pedestrian**, with clear view of the sea, expecting to get wet	0.1
Trained staff expecting to get wet, low danger of fall from the walkway	1 - 10
Sinking small boats set 5 – 10 m from structure; damage to larger yachts	10
Significant damage or sinking of larger yachts	50
Damage to **paved promenade** behind seawall	200
Structural damage to **seawall** crest	200

8.2 Tests Results

The results of overtopping assessment for the study are presented in Table 8.2. As discussed in Section 4, onshore winds which would likely occur concurrently with the design waves would increase the overtopping rates over those tested. It is standard industry practice for physical modelling tests to only consider the overtopping rate due to waves, with no consideration of the additional effects of wind (due to the unnecessary level of complexity and cost that would be required to include wind effects).

Table 8.2: Overtopping Results for Upgrades 8 and 9 (Prototype Scale)

Upgrade #	Event	Water Level (m AHD)	H_s (m)	T_p (s)	Chainage (m)	Ave. Overtopping Rate (L/s/m)
8	10 year ARI HAT	1.2	4.8	12.5	400-500	0.23
					500-600	0.51
					600-700	0.84
					700-800	0.07
8	100 year ARI HAT + SLR	1.9	5.5	15.1	400-500	6.79
					500-600	5.52
					600-700	9.93
					700-800	1.07
9	10 year ARI HAT	1.2	4.8	12.5	400-500	0.28
					500-600	1.48
					600-700	2.68
					700-800	0.27
9	100 year ARI HAT + SLR	1.9	5.5	15.1	400-500	1.23
					500-600	7.18
					600-700	15.25
					700-800	4.82

While the two different upgrade design were not tested specifically for the 2004 historical event, it was possible to compare the improvement in overall overtopping performance for both Upgrades 8 and 9 with the existing breakwater design with the results of the 10 year ARI tests. Both upgrade designs lowered the average overtopping rates to below 3 L/s/m for the 10 year ARI HAT event, reducing the associated hazard to pedestrian hazard only (conditions not considered hazardous for the breakwater or other infrastructure).

As expected, it was observed that the reduction in rock berm width, from 10 m to 5 m, between Upgrade 8a and Upgrade 8b, resulted in an increase in average overtopping rates. On average and between ch. 500 m and ch. 800 m, overtopping rates were observed to increase by nearly 60% for the 10 year ARI HAT event and by 25% for the 100 year ARI HAT+SLR event, as a result of the reduced rock berm width.

For both designs, the peak intensity overtopping was observed to occur along the central section of the breakwater (ch. 500 m to ch. 700 m). Large waves were still observed to generate high vertical spray when breaking on the seaward slope of the breakwater. Under certain conditions, the breaking waves were observed to generate overtopping jets which would have impacted the crest access way and possibly the leeward slope. It should also be noted that on one occasion during the 100 year ARI event, overtopping was observed to dislodge a 3 t rock from the rock armoured slope at approximately ch. 450 m, and carry it across the crest access way. It should be noted that the mass of this displaced rock is below the M_{15} of the rock mass distribution used for the 5-8 tonne rock berm.

9. Summary and Conclusions

9.1 Overview

WRL was commissioned by GHD to undertake 3D physical model testing of remedial design upgrades to the Coffs Harbour Northern Breakwater. The key objectives of the 3D physical model study included:

- Validation of the model for the existing breakwater using two previous storm events that have occurred;
- 3D armour stability assessment of the different design upgrades to the existing breakwater;
- Quantitative overtopping assessment of the different design upgrades to the existing breakwater; and
- Optimisation of the upgrade design to minimise wave overtopping of the breakwater.

9.2 Model Layout and Test Conditions

A detailed description of the wave basin layout was included in Section 4. The layout of the 1:58 scale 3D model within the wave basin is shown in Figure 4.3, with the bathymetry at the site modelled seaward of the existing breakwater for a distance of approximately 600 m.

The model of the existing breakwater was qualitatively validated for two previous storm events (2004 and 2009), and breakwater upgrade options were tested for 10 year ARI and 100 year ARI swell wave events. All testing was undertaken with a representative wave direction of 62.5º TN at the model's seaward (eastern) boundary.

9.3 Summary of Results

9.3.1 Historical Validation

Model validation testing involved a qualitative assessment of the overtopping processes along the existing breakwater in areas where this is known to be a major hazard. This was performed for the following two (documented) recent storm events:

- 6th March 2004; and
- 22nd May 2009.

The model validation was based on a visual comparison of overtopping experienced during the previous storm events on the real world breakwater (captured in photographs), with observations from multiple vantage points during basin modelling of the same events. This process determined that the physical model was reproducing the nearshore wave and overtopping processes reasonably well for the existing breakwater structure, such as scale of the vertical spray as well as the submergence extent along the crest under large waves. Analysis of measured average overtopping rates showed that the values recorded during model testing matched the hazard rating of these two events by Watterson and Driscoll (2011).

9.3.2 Armour Stability Tests

Two breakwater upgrade design options were considered in the physical model program:

- Upgrade 8, consisting of a composite Hanbar armoured upper slope and 10 m wide rock berm; and
- Upgrade 8b, consisting of a composite Hanbar armoured upper slope and 5 m wide rock berm.

Primary armour, crest specific armour units, as well as rock berm armour stability for the proposed breakwater upgrade designs were investigated under 10 year ARI (HAT) and 100 year ARI (HAT + SLR) wave conditions.

In general, both upgraded breakwater designs were considered stable and suffered very low overall damage (less than 1%). The rock berm was observed to exhibit some slight reshaping behaviour but with overall negligible damage. It was observed that the reduced rock berm width of Option 8b resulted in slightly higher damage to the 12 t Hanbars and rock berm when compared with Option 8a.

9.3.3 Overtopping Tests

Overtopping tests were performed for the two different breakwater upgrade designs for both 10 year ARI (HAT) and 100 year ARI (HAT+SLR) events. Quantitative overtopping assessment was performed over 400 m of crest length for the upgraded breakwater. Overtopping of the breakwater was assessed for discretised adjacent 100 m long (prototype scale) sections in order to provide information regarding the distribution of overtopping and assist in identifying sections of breakwater with higher overtopping risk.

Both breakwater upgrade designs were observed to significantly lower the average overtopping rates compared with the existing breakwater, with overtopping rates below 3 L/s/m for the 10 year ARI HAT event, reducing the associated hazard to a pedestrian hazard only. The reduction in rock berm width from 10 m to 5 m, between Upgrade 8a and Upgrade 8b, resulted in an increase in average overtopping rates. On average and between Ch. 500 m and 800 m, overtopping rates were observed to be almost 60% higher for the 10 year ARI (HAT) event and 25% higher for the 100 year ARI (HAT+SLR) event for Upgrade 8b compared to Upgrade 8.

10. References

Broderick, L and Ahrens, J P (1982), *Rip-Rap Stability Scale Effects*, Technical Paper 82-3, US Army Engineer Waterways Experiment Station, Vicksburg, MS.

CEM (2003), *Coastal Engineering Manual*, Engineer Manual 1110-2-1100, Volumes 1-7, Coastal Engineering Research Center, Waterways Experiment Station, US Army Corps of Engineer, Vicksburg, USA.

CIRIA, CUR, CETMEF (2007), *The Rock Manual. The use of Rock in Hydraulic Engineering (2nd Edition).* C683, CIRIA, London.

Dai, Y B and Kamel, A M (1969), *Scale Effect Tests for Rubble Mound Breakwaters*, US Army Engineer Waterway Experiment Station, Corps of Engineers, Vicksburg, Mississippi, Research Report H-69-2 (1969).

Dalrymple, R A (1985), *Introduction to Physical Models in Coastal Engineering,* In Physical Modelling in Coastal Engineering, R.A. Dalrymple (ed.), A.A. Balkema, Rotterdam.

GHD (2014), *Coffs Harbour Northern Breakwater Upgrade Options Multi-Criteria Analysis Report,* Report prepared for NSW Department of Primary Industries – Catchments and Lands.

Jensen, O J and Klinting, P (1983), *Evaluation of Scale Effects in Hydraulic Models by Analysis of Laminar and Turbulent Flows*, Coastal Engineering 7.

Hughes, S A (1993), *Physical Models and Laboratory Techniques in Coastal Engineering*, Advanced Series in Ocean Engineering – Volume 7, World Scientific, Singapore.

Hydralab III (2007), *Guidelines for Physical Model Testing of Breakwaters: Rubble Mound Breakwaters,* Deliverable NA3.1-2, European Community, Final Version 1.3, August 2007.

Manly Hydraulic Laboratory [MHL] (2004), *North Breakwater Asset Appraisal Physical Model Report*, Report MHL 1196, December 2004.

Mansard and Funke (1980), *The Measurement of Incident and Reflected Spectra Using a Least Squares Method*, 17th International Conference on Coastal Engineering, American Society of Civil Engineers, USA.

Mol, A, Ligteringen, H, Groeneveld, R L and Pita, C R (1983), "West Breakwater – Sines: Study of Armour Stability", *Proceedings of Coastal Structures '83*, American Society of Civil Engineers, pp 57-70.

SPM (1984), *Shore Protection Manual*, US Army Coastal Engineering Research Center, Vicksburg, Mississippi, USA.

Tirindelli, M, Lamberti, A, Paphitis, D, Collins, M, Vidal, C, Hawkins, S, Moschella, P, Burcharth, H, Sanchez-Arcilla, A, (2000), *Wave Action on Rubble Mound Breakwaters: the Problem of Scale Effects*, DELOS EVK3-CT-2000-00041.

Tørum, A, Mathiesen, B and Escutia, R (1979), *Reliability of Breakwater Model Tests,* Proceedings of Coastal Structures Conference 1979, American Society of Civil Engineers, pp. 454-469.

U.S. Army Corps of Engineers (2006), Coastal engineering manual. Engineer Manual 1110-2-1100, U.S. Army Corps of Engineers, Washington, D.C. (in 6 volumes).

Van der Meer, J W (1988), *Rock Slopes and Gravel Beaches Under Wave Attack*, Ph.D Dissertation, Delft Hydraulics Communication No. 396, Delft Hydraulics Laboratory, Emmeloord, The Netherlands.

Watterson, E, Driscoll, S (2011), *Reducing Public Safety Risk at NSW Breakwater*, 20th NSW Coastal Conference, Australia.

Appendix A – Upgrade 8a 2D Laser Surveys

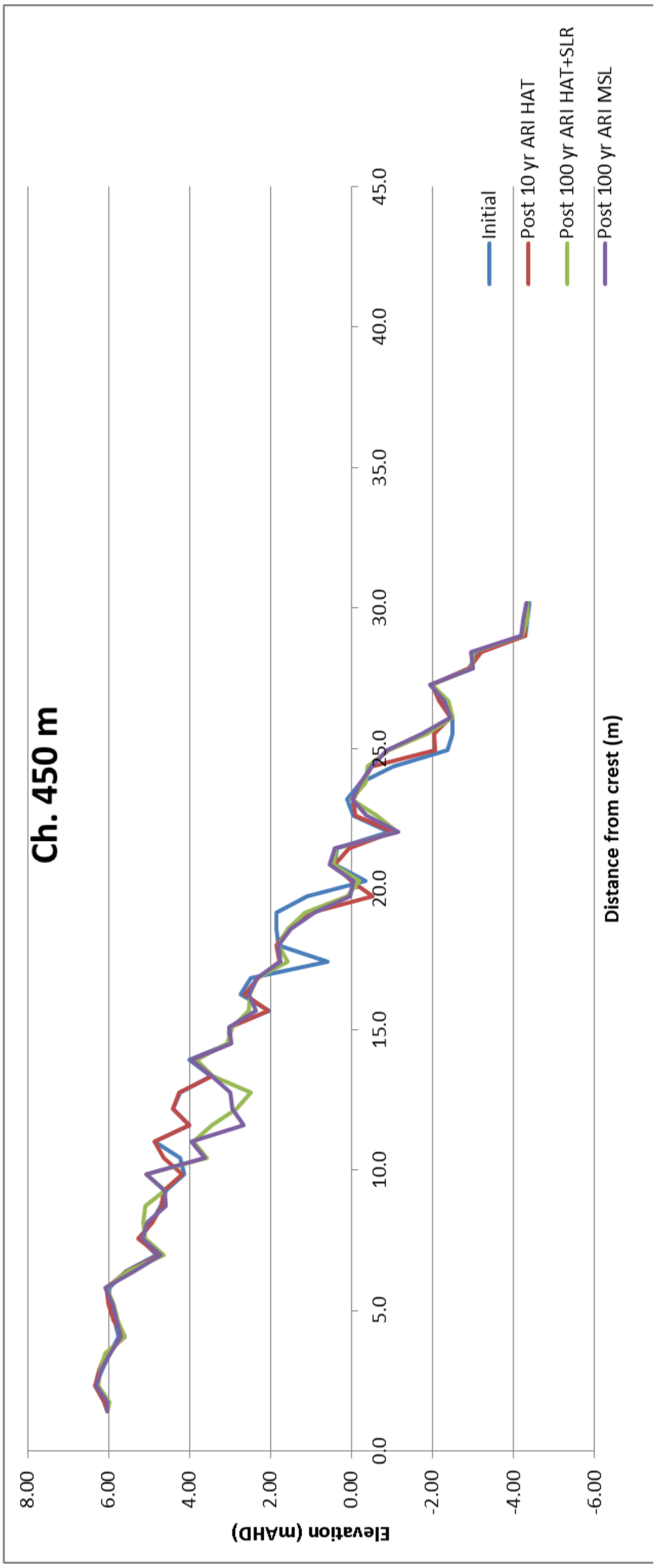

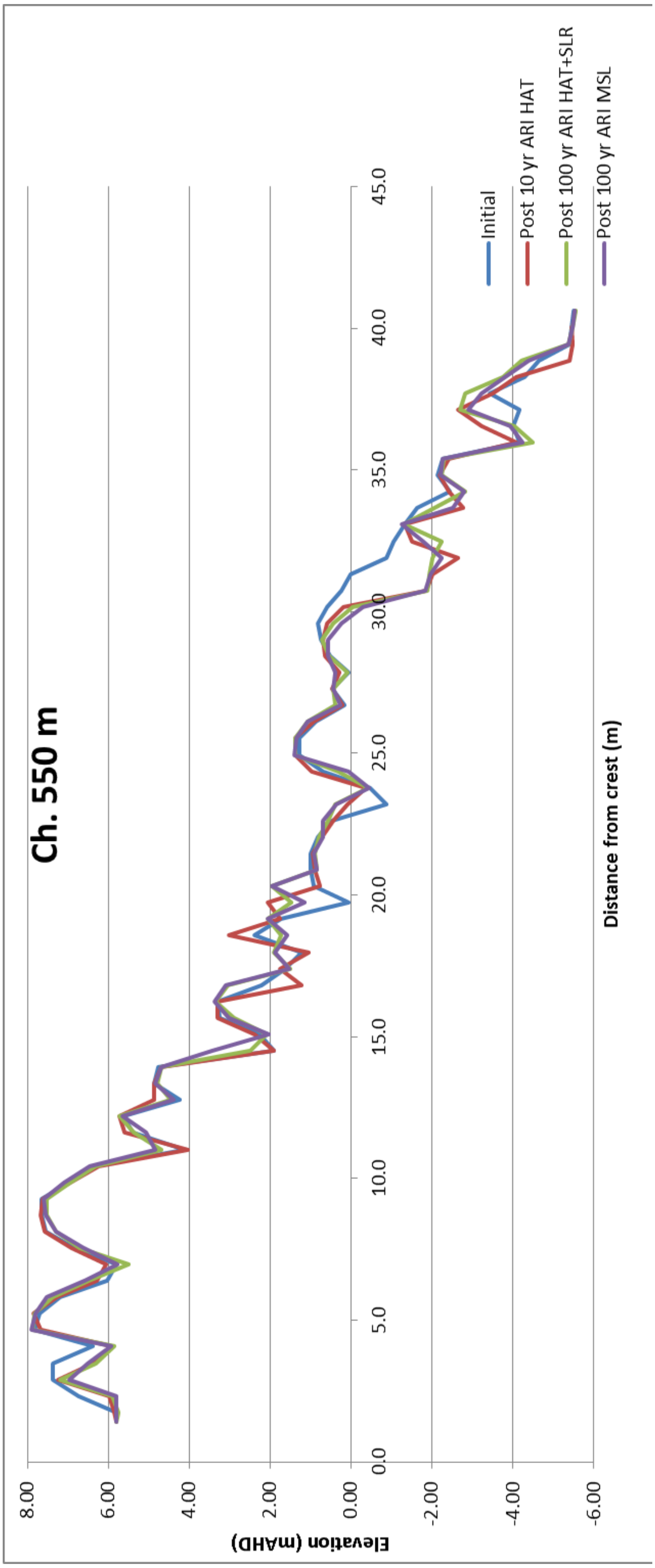

Ch. 550 m
Elevation (mAHD)
8.00
6.00
4.00
2.00
0.00
-2.00
-4.00
-6.00
0.0
5.0
10.0
15.0
20.0
25.0
30.0
35.0
40.0
45.0
Distance from crest (m)
Initial
Post 10 yr ARI HAT
Post 100 yr ARI HAT+SLR
Post 100 yr ARI MSL

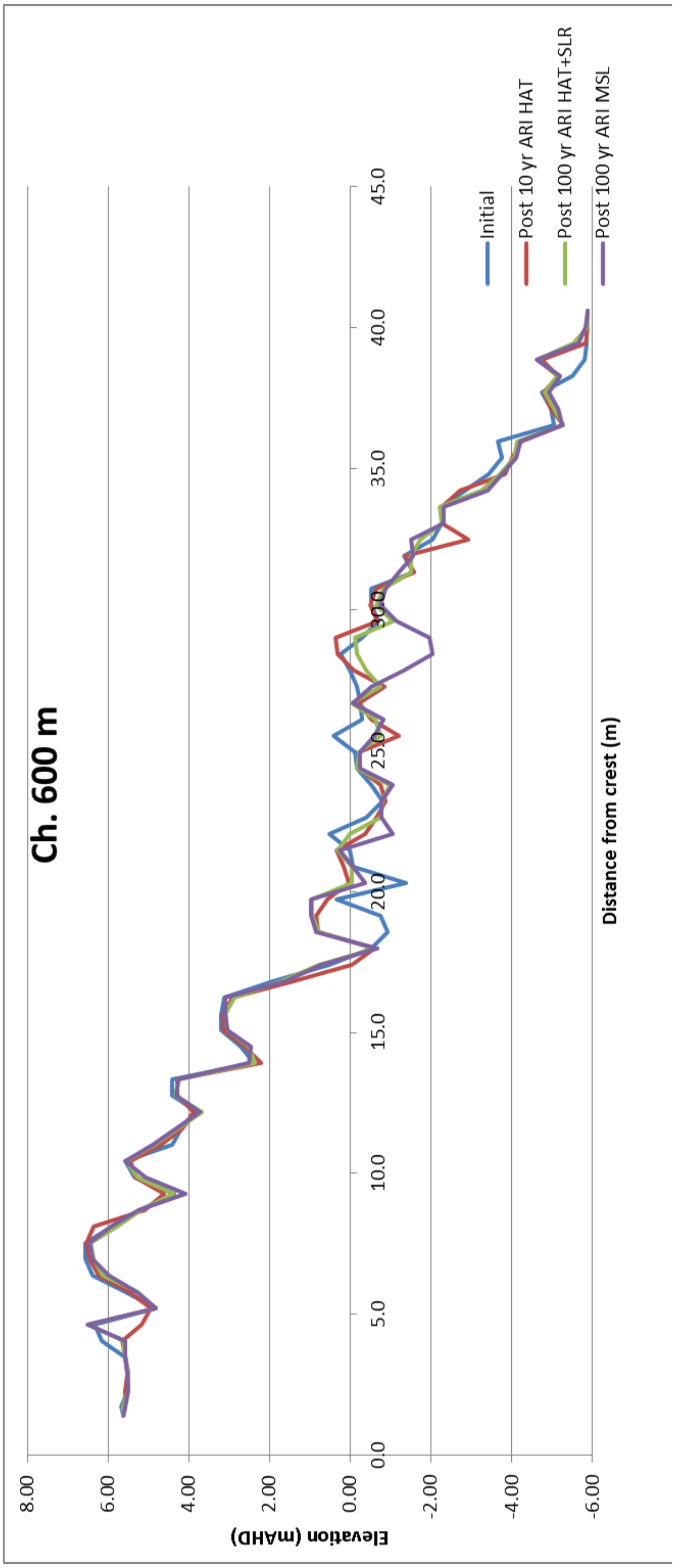
Ch. 600 m
Elevation (mAHD)
8.00
6.00
4.00
2.00
0.00
-2.00
-4.00
-6.00
0.0
5.0
10.0
15.0
20.0
25.0
30.0
35.0
40.0
45.0
Distance from crest (m)
Initial
Post 10 yr ARI HAT
Post 100 yr ARI HAT+SLR
Post 100 yr ARI MSL

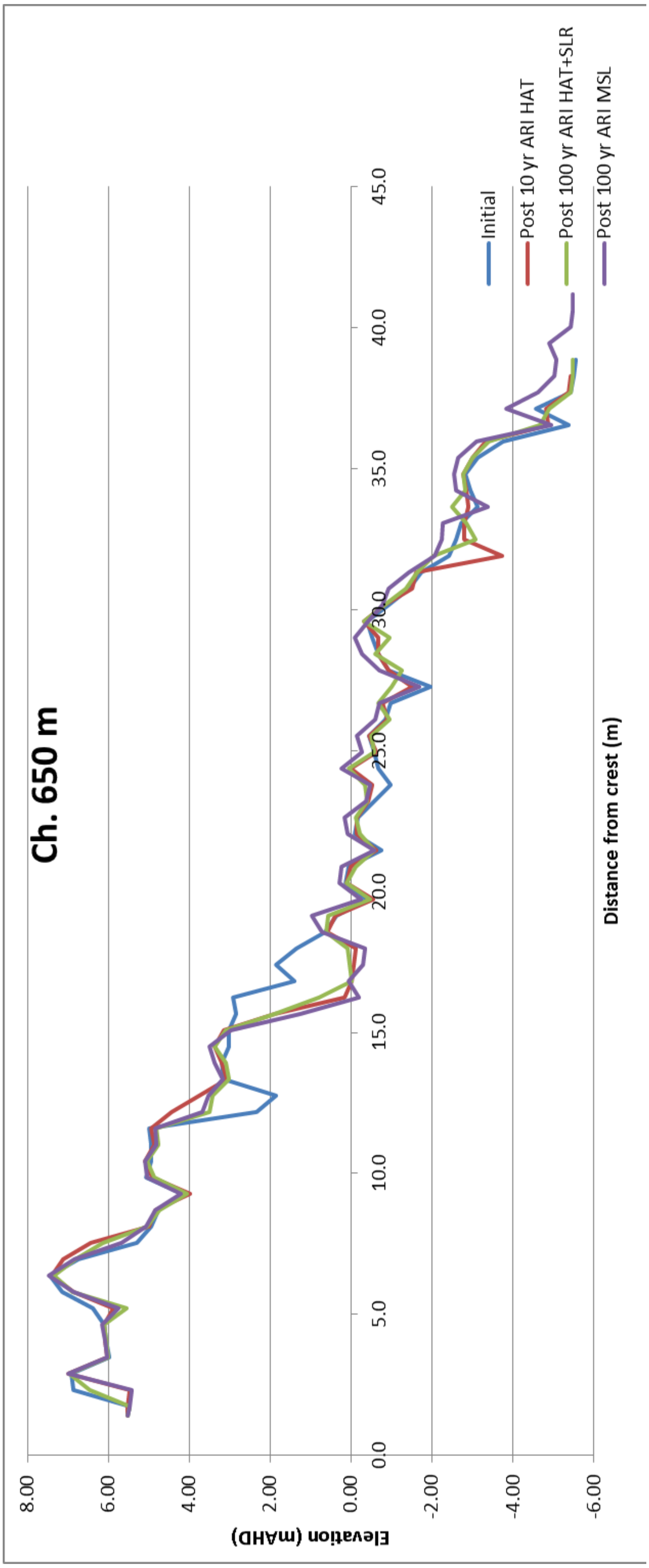
Ch. 650 m
Elevation (mAHD)
Distance from crest (m)
Initial
Post 10 yr ARI HAT
Post 100 yr ARI HAT+SLR
Post 100 yr ARI MSL
8.00
6.00
4.00
2.00
0.00
-2.00
-4.00
-6.00
0.0
5.0
10.0
15.0
20.0
25.0
30.0
35.0
40.0
45.0

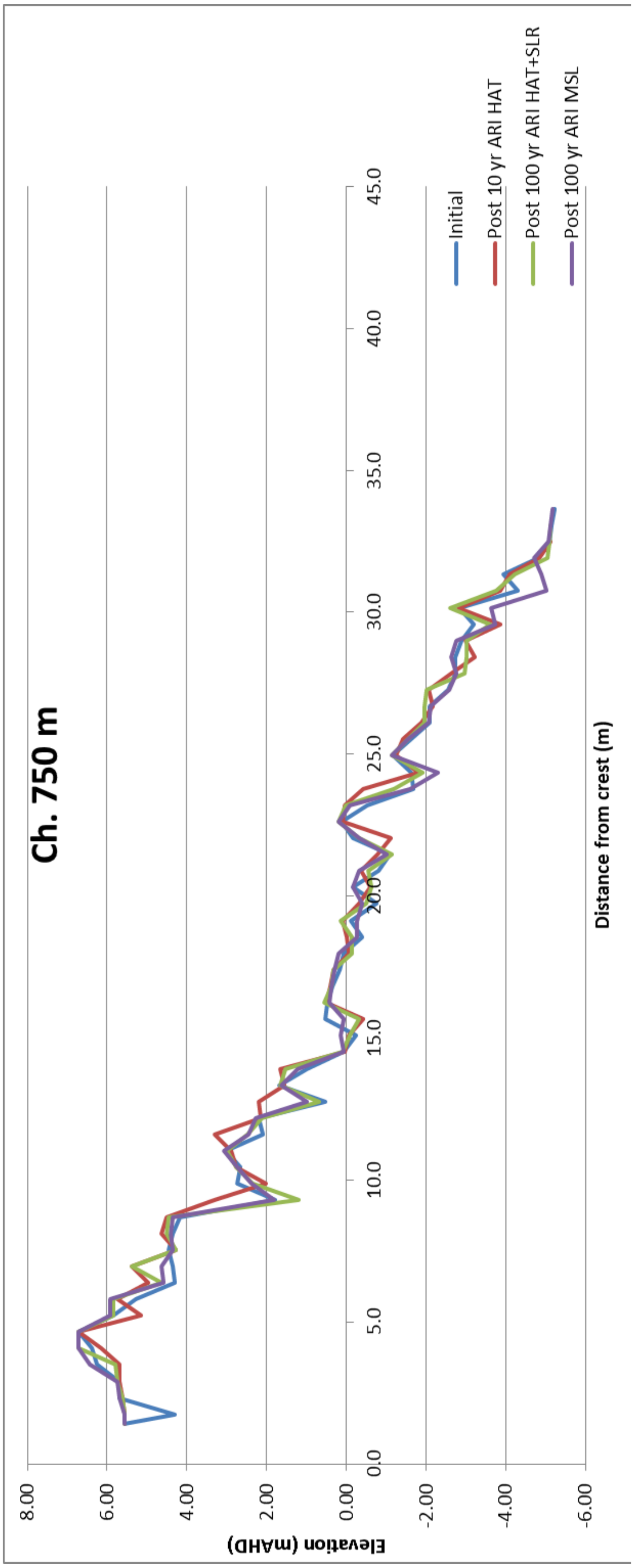

Ch. 750 m
Elevation (mAHD)
Distance from crest (m)
Initial
Post 10 yr ARI HAT
Post 100 yr ARI HAT+SLR
Post 100 yr ARI MSL

Appendix B – Upgrade 8b 2D Laser Surveys

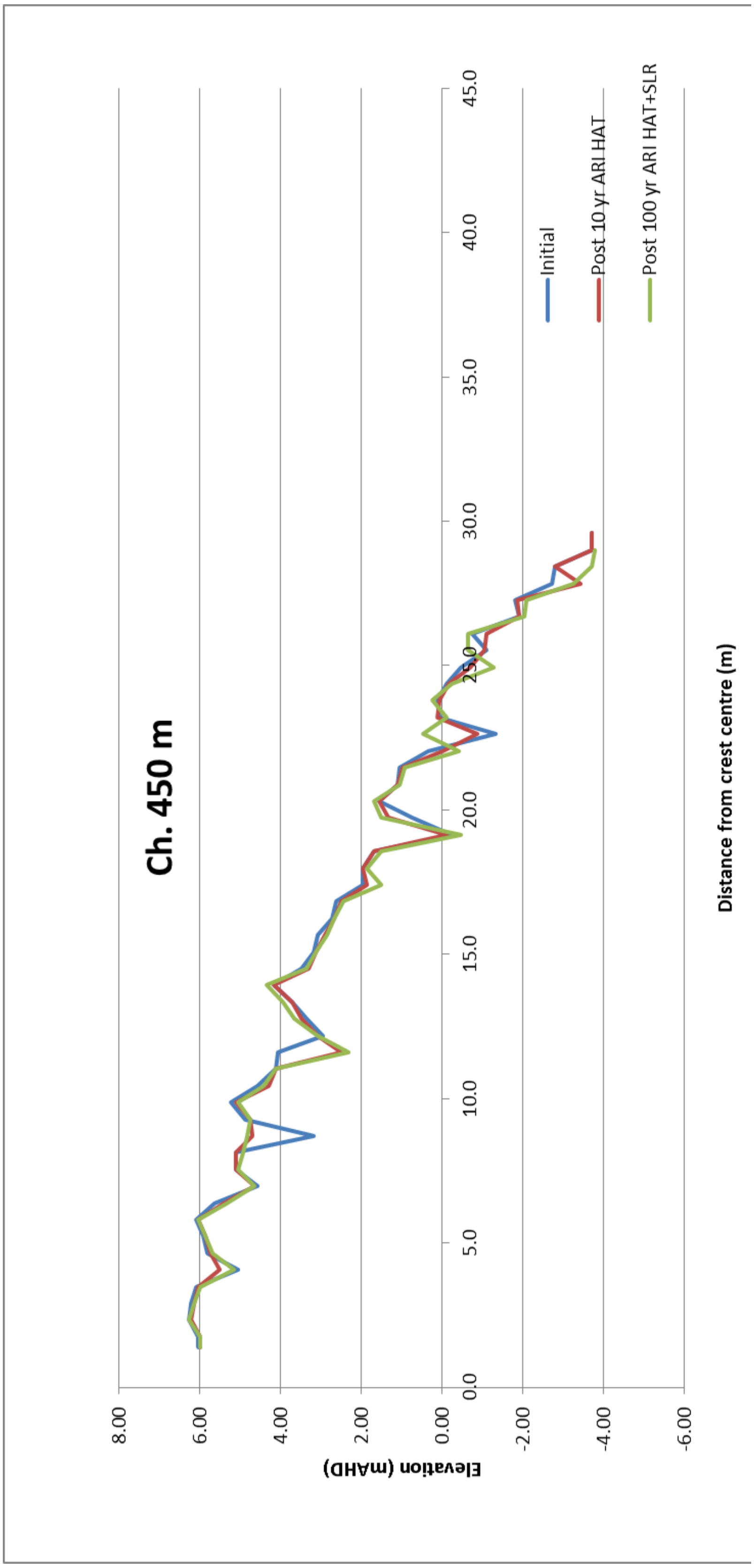

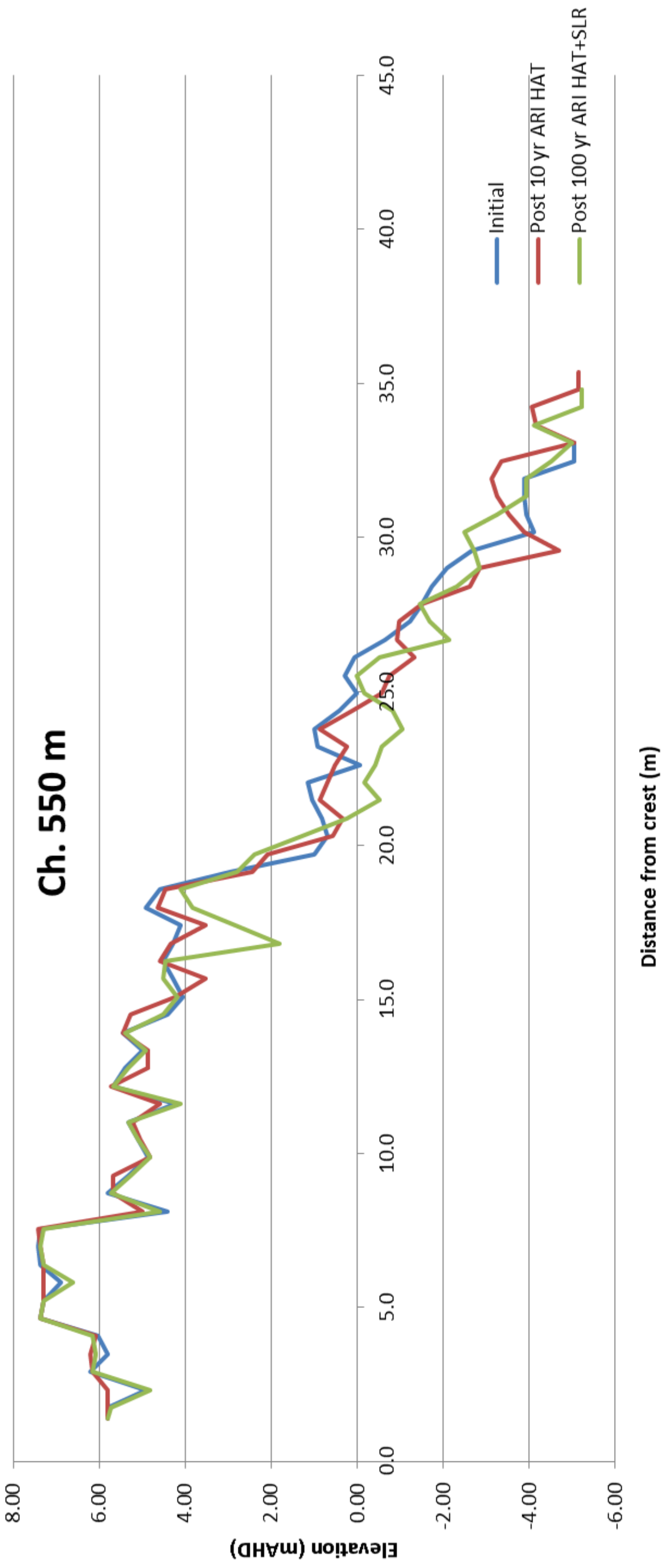
Ch. 550 m
Elevation (mAHD)
8.00
6.00
4.00
2.00
0.00
-2.00
-4.00
-6.00
Distance from crest (m)
0.0
5.0
10.0
15.0
20.0
25.0
30.0
35.0
40.0
45.0
Initial
Post 10 yr ARI HAT
Post 100 yr ARI HAT+SLR

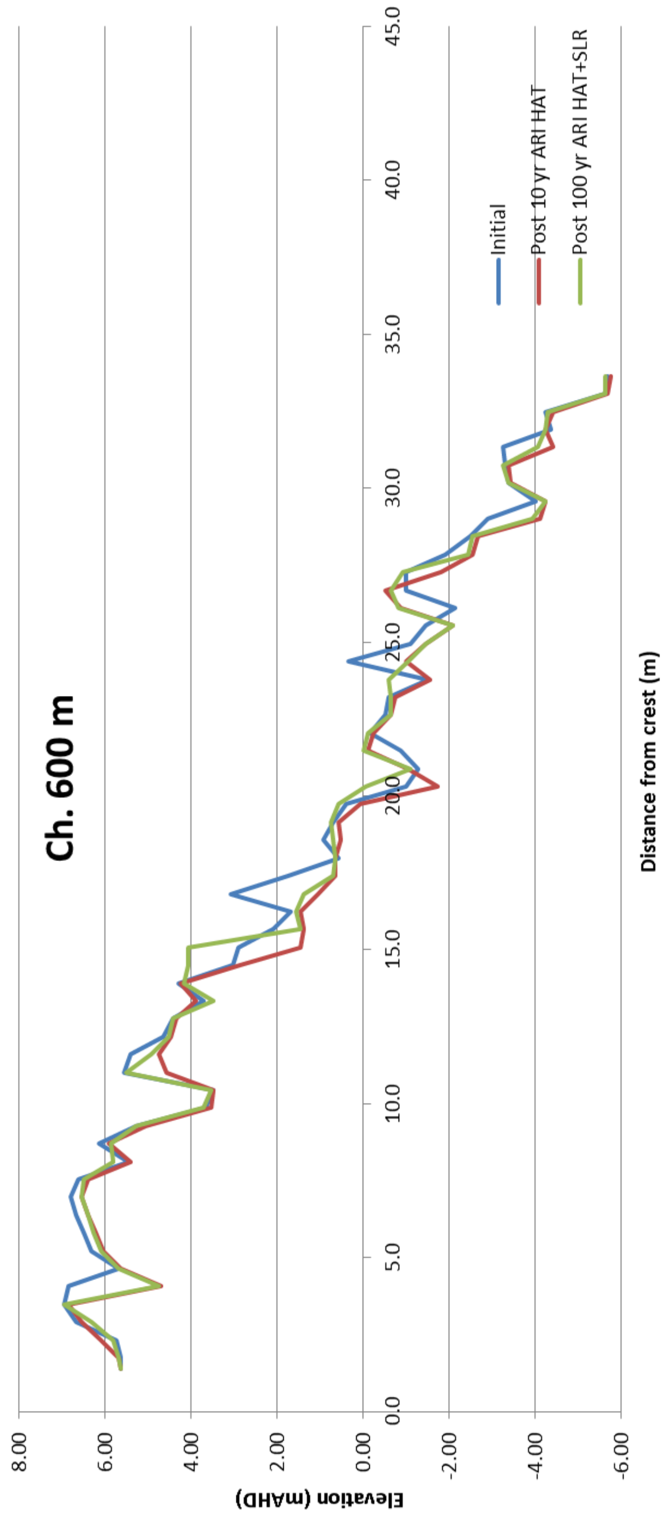
Ch. 600 m
Elevation (mAHD)
Distance from crest (m)
8.00
6.00
4.00
2.00
0.00
-2.00
-4.00
-6.00
0.0
5.0
10.0
15.0
20.0
25.0
30.0
35.0
40.0
45.0
Initial
Post 10 yr ARI HAT
Post 100 yr ARI HAT+SLR

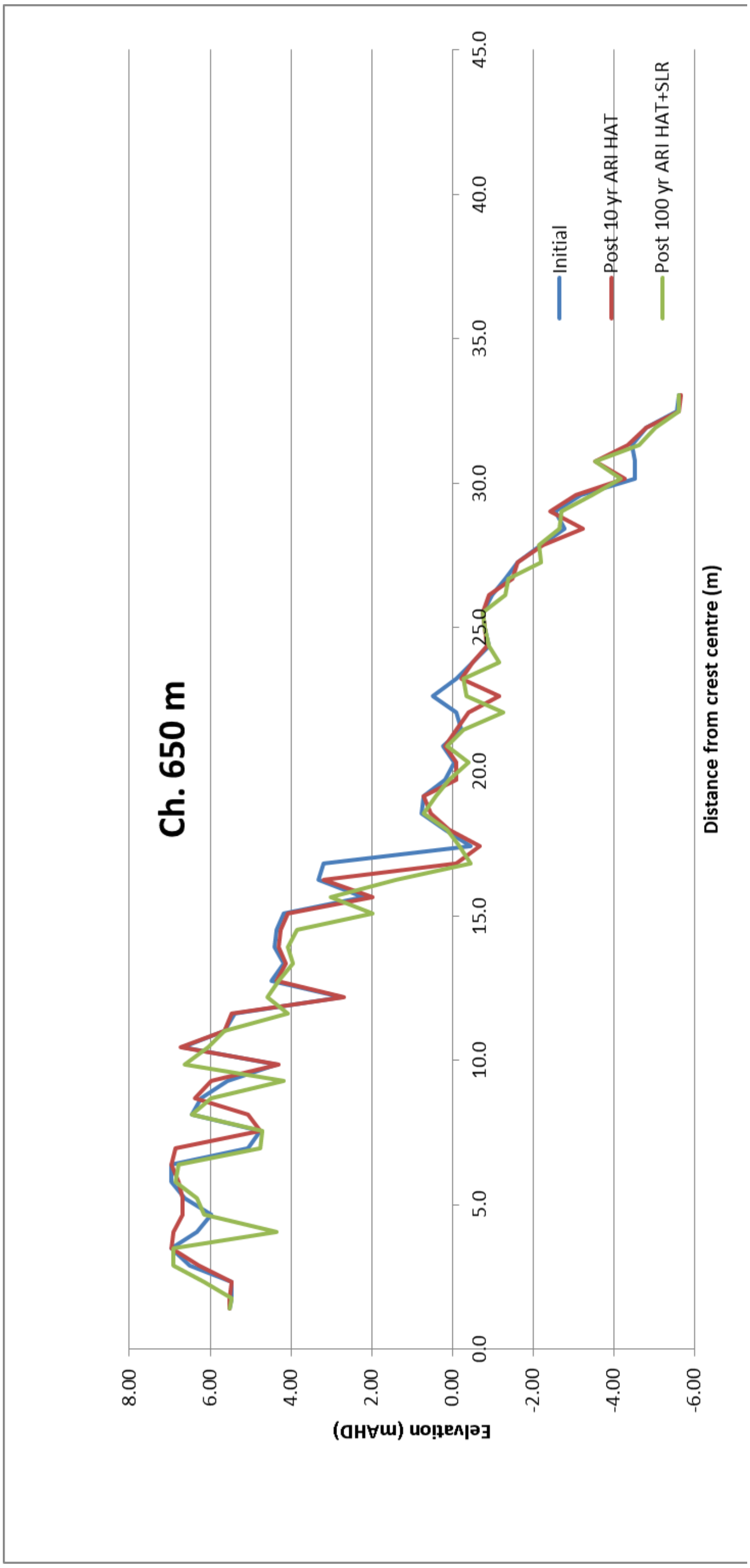

Ch. 650 m
Elevation (mAHD)
Distance from crest centre (m)
Initial
Post 10 yr ARI HAT
Post 100 yr ARI HAT+SLR

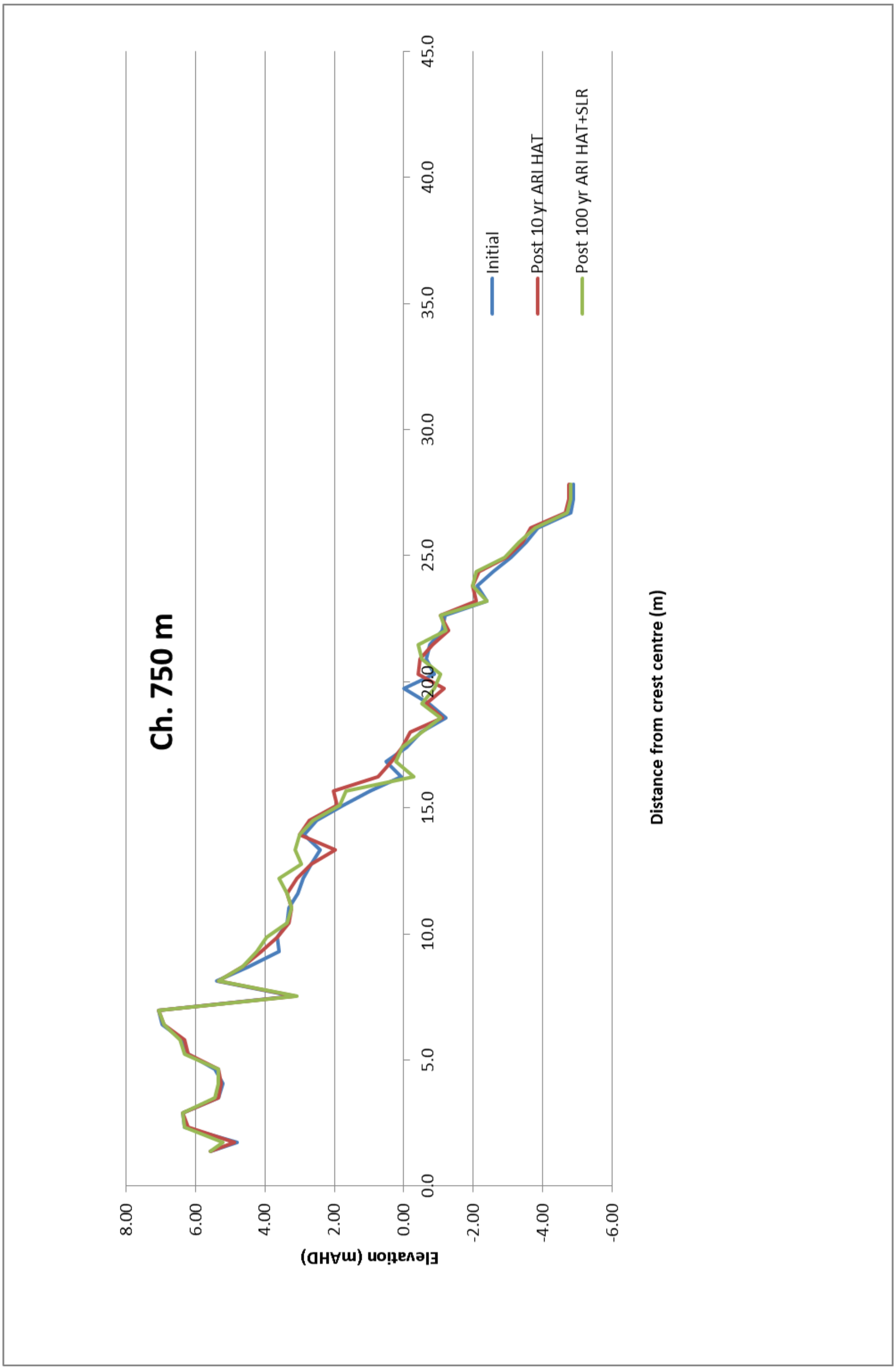
Ch. 750 m
Elevation (mAHD)
8.00
6.00
4.00
2.00
0.00
-2.00
-4.00
-6.00
0.0
5.0
10.0
15.0
20.0
25.0
30.0
35.0
40.0
45.0
Distance from crest centre (m)
Initial
Post 10 yr ARI HAT
Post 100 yr ARI HAT+SLR